TAMPERE UNIVERSITY OF TECHNOLOGY

SANTTU KOSKINEN

ANALYSIS OF INKJET-PRINTED FLEX-MODULE IN A MOBILE PHONE

Master of Science Thesis

The subject was approved by the Faculty Council of Computing and Electrical Engineering
June 8th 2011
Examiners: Prof. Jukka Vanhala, Dr. Matti Mäntysalo

ABSTRACT

TAMPERE UNIVERSITY OF TECHNOLOGY
Master's Degree Programme in Electrical Engineering
SANTTU KOSKINEN: Analysis of Inkjet-printed Flex-module in a Mobile Phone
Master of Science Thesis, 63 pages, 14 Appendix pages
October 2011
Major: Electronics
Examiners: Prof. Jukka Vanhala, Dr. Matti Mäntysalo
Keywords: flexible electronics, inkjet, printable electronics, electronics manufacturing technology, laser processing

Flexible circuit boards are becoming more and more common in small and lightweight consumer electronics devices. Manufacturers are seeking novel technologies for flexible circuit manufacturing. Cost-efficiency, environmental effects of the manufacturing technology and reducing process steps in manufacturing are the key drivers for development. Printed electronics, especially inkjet technology, has been an emerging viable candidate for flexible circuit board manufacturing over the last few years. Additive processing, minimal material consumption and digitally guided processing are the main attractors of inkjet printing technology.

The objective of this thesis work is to demonstrate a flexible circuit board of a commercial mobile phone with inkjet printing technology. The design of the flexible printed circuit board is transferred to inkjet printing technology. The assembly process of the flex module is presented, including laser processing of the substrate, inkjet printing of the circuit layout, component attachment using isotropically conductive adhesive and epoxy and circuit coating. The end result is a flexible circuit, similar to the original design, produced with a new manufacturing technology. The inkjet printed demonstrators were then electrically tested by the original manufacturer of the device. Testing showed that functional prototypes with close to the same performance of the original devices were manufactured.

The target of the thesis work was reached. Functional demonstrators with good performance were manufactured with inkjet printing technology. As other outcome knowledge of manufacturing electronics with inkjet printing was further increased, as methods for the design and assembly phase were developed. A specific image masking algorithm for processing of the inkjet printer bitmap images was introduced in the device design phase. Method for making vias on substrate with inkjet printing technology was demonstrated. Also a method for component attachment on flexible inkjet printed circuits was demonstrated.

TIIVISTELMÄ

TAMPEREEN TEKNILLINEN YLIOPISTO
Sähkötekniikan koulutusohjelma
SANTTU KOSKINEN: Matkapuhelimessa käytettävän inkjet-tulostetun taipuisan piirilevyn analyysi
Diplomityö, 63 sivua, 14 liitesivua
Lokakuu 2011
Pääaine: Elektroniikka
Tarkastajat: Prof. Jukka Vanhala, Matti Mäntysalo, TkT
Avainsanat: taipuisa elektroniikka, inkjet, painettava elektroniikka, elektroniikan valmistustekniikka, laserprosessointi

Kuluttajaelektroniikkalaitteiden koon pienentyessä taipuisat piirilevyt tulevat jatkuvasti yleisimmiksi laitteiden rakenteissa. Valmistajat pyrkivät kehittämään piirilevyn valmistusprosesseja jatkuvasti. Ajureina toimivat mm. valmistuksen ja materiaalien hinta, ympäristönäkökulmat, sekä valmistuksessa käytettävien prosessivaiheiden määrän vähentäminen. Painettavan elektroniikan eri osa-alueet, erityisesti inkjet-teknologia, ovat pyrkineet viime vuosina tarjoamaan vaihtoehdon perinteisille taipuisien piirilevyjen valmistusprosesseille. Inkjet teknologian houkuttelevina puolina nähdään prosessin additiivisuus, vähäinen materiaalinkulutus, sekä digitaalisesti ohjattu valmistusprosessi.

Tämän opinnäytetyön tavoitteena on osoittaa inkjet-teknologian soveltuvuus taipuisien piirilevyjen valmistukseen demonstraattorilaitteen kautta. Matkapuhelimessa käytettettävän taipuisan piirlevyn sunnittelutiedostoja muokkaamalla piirilevyn valmistustiedostot siirrettiin inkjet-teknologialla toteutettaviksi. Työssä käydään läpi valmistusprosessin eri vaiheet, kuten piirilevyn ulkoreunojen ja läpivientien laserleikkaus, johdotuskerrosten inkjet-painaminen, komponenttien liittäminen isotrooppisesti johtavalla liimalla ja epoksilla, sekä piirilevyn päällystäminen suojauslakalla. Lopputuloksena on alkuperäisen kaltainen, uudella valmistusteknologialla valmistettu taipuisa piirilevy. Valmistetut prototyypit testattiin alkuperäisen valmistajan toimesta. Testausvaiheen päätelmänä voidaan todeta, että toimivia taipuisia piirilevy valmistettiin inkjet-teknologiaa hyväksikäyttäen ja valmistetut piirilevyt vastasivat sähköiseltä suorituskyvyltään suurilta osin alkuperäistä tuotetta.

Työlle asetettu tavoite saavutettiin. Toimivia taipuisia piirilevyjä valmistettiin inkjet-teknologiaa hyväksikäyttäen. Asetetun tavoitteen lisäksi työstä saatiin irti myös muuta hyödyllistä tietoa inkjet-teknologian käytöstä elektroniikan valmistuksessa. Sekä suunnittelu-, että valmistusvaiheessa käytettiin uusia menetelmiä. Kuvanmaskausalgoritmi mahdollisti tarkkojen rakenteiden tulostamisen. Piirilevyn läpiviennit valmistettiin käyttäen hyväksi laserleikkausta ja inkjet-teknologiaa, sekä työssä esitettiin eräs menetelmä komponenttien liittämiseen taipuisaan piirilevyyn.

PREFACE

This M.Sc. work was done at the Department of Electronics at Tampere University of Technology. The thesis work was carried out as a part of PIPA project which is a collaborative project funded by Meadville, Nokia, Premix, Tekes (Finnish Funding Agency for Technology and Innovation), Tampere University of Technology, University of Oulu and UPM.

I would like to thank the thesis work examiners Professor Jukka Vanhala and Doctor Matti Mäntysalo for guidance during the thesis work. In addition, I would like to thank Lasse Pykäri, Ying-Maria Dong and all other related personnel of Nokia for the help and support during this work.

I would also like to thank my present and former colleagues in the TUT Printable Electronics Group for ideas, fruitful conversations and support during the thesis work.

Lastly, I would like to thank my family and my friends for the support during this thesis work.

Tampere, Finland
October, 2011 Santtu Koskinen

TABLE OF CONTENTS

LIST OF NOTATION AND ABBREVIATIONS

dBm	Difference in decibels to one milliwatt
dBr	Difference in decibels to a specified reference level
dBμV/m	Difference in decibels to one microvolt per meter
DOD	Drop on demand
DPI	Dots per inch
DUT	Device Under Test
EIRP	Effective Isotropic Radiated Power
EMC	Electromagnetic compatibility
ESD	Electrostatic discharge
FPC	Flexible printed circuit
HF	High Frequency
Gerber	A file format used in PCB manufacturing industry
ICA	Isotropically conductive adhesive
LCD	Liquid Crystal Display
LED	Light Emitting Diode
PCB	Printed circuit board
RE	Radiated Emissions
RF	Radio Frequency
RSE	Radiated Spurious Emissions
RX	Receive
SMT	Surface Mount Technology
SPR	Standard Product Requirements
TA	Type Approval
TDMA	Time Division Multiple Access
TIS	Total Isotropic Sensitivity
TIFF	Tagged image file format
TRP	Total Radiated Power
TX	Transmit

1. INTRODUCTION

Consumer electronics devices tend to become ever smaller and lighter. One way of reducing the size and weight of an electronics device is to use flexible circuit boards in devices, such as mobile phones, cameras and laptop computers. Usually the reason for using a flexible circuit in the device body is a need for reduction in device size and weight, a need for placing the circuit on a non-flat surface or a movable property needed in the device structure. Flexible circuits can be used to wrap a circuit around a device body in a stationary application, or to provide a hinge or a joint between moving parts in a dynamic application.

The drivers for seeking new manufacturing technologies to produce flexible circuits are many. Cost-efficient materials, environmental values and fewer process steps in manufacturing are preferred. Inkjet printing is an emerging technology which can be used for making flexible electronics. The variety of materials which can be deposited using inkjet technology is constantly expanding. Conductive materials [1], dielectrics [2] [3] and organic semiconductors [4] have been printed using inkjet technology. Manufacturing printed circuit boards by inkjet technology differs from the common manufacturing methods in some ways. Because inkjet technology is an additive process, the material waste in the manufacturing stage is minimal. All deposited material is used for the creation of the circuit as no material is taken away. In large scale manufacturing, this could have a positive environmental impact. Digital control of the printing process [5] enables easy and fast modifications to circuit board layout files, which is beneficial for e.g. prototyping and small volume manufacturing purposes.

The objective of this thesis work is to demonstrate the applicability of inkjet printing for manufacturing of flexible circuits through a demonstrator case. Circuit design of a flexible circuit board of a mobile phone was taken and transferred for inkjet printing technology. A set of prototypes were manufactured by inkjet printing and their functionality was verified by electrical tests. This thesis covers the design modification, assembly and testing phases of a demonstrator manufactured by inkjet technology.

In chapter two traditional flexible circuit manufacturing technologies are briefly discussed and compared with inkjet printing. The focus is on the manufacturing on a two-sided flexible circuit because of the demonstrator device. The idea is to

give the reader sufficient background to understand the characteristics of common manufacturing methods and inkjet printing technology.

In chapter three the demonstrator case is introduced. The material selection and the steps of transferring the design files to inkjet printing technology are gone through. Modifications to the design files are discussed and a masking algorithm for improving printed image quality is presented.

In chapter four the assembly phase of the demonstrator prototypes is gone through. Substrate preparations, laser processing of the module outline and vias, inkjet printing of the circuit board, component attachment and circuit coating methods are discussed in detail.

Chapter five covers the testing phase and analysis of the test results. Details of the manufactured prototypes are compared with the original flex module with the help of cross-sectional images. Test procedures and results of electromagnetic compatibility (EMC) test, electrostatic discharge (ESD) test, antenna test, display test and audio test are discussed. Chapter six describes the future development that is to be carried out with the demonstrator case, but is not to be included in this thesis work. In chapter seven final conclusions of the entire project are drawn.

2. FLEXIBLE ELECTRONICS

The term flexible electronics is very wide and its meaning is constantly expanding due to progress and new innovations made in the industrial and research fields. Today the term covers areas such as flexible displays, flexible solar cells, flexible sensors, flexible thin-film transistor circuits and flexible circuits among other areas [6]. In this chapter the focus is on the characteristics and manufacturing of flexible circuits. Making flexible circuits by conventional means and by inkjet-printing are discussed.

2.1 Flexible Circuits

The history of flexible circuits dates back to the turn of the 20th century. Patents issued at that time show that researchers were developing ways to make flexible interconnections for example in telephony and military applications. During World War II flexible circuits were adopted to military applications such as the German made V2 rocket [7]. Later on flexible circuits have become essential part of every day electronic devices such as desktop printers, cameras, computers and mobile phones. Today flexible circuit industry is a vast global market with countries like Japan and USA holding the most significant market shares. [7]

The IPC-T-50 industry standard "Terms and Definitions for Printed Boards." defines flexible circuit as "A patterned arrangement of printed wiring utilizing flexible base material with or without flexible cover layers". The definition is broad as is the variety of flexible circuit types. The applications for flexible circuits are many but these applications can be roughly divided into static and dynamic applications. In a static application the flexibility of the circuit is needed when installing the circuit in the application but no actual flexibility is needed during the use of the device. One example of a static flexible circuit application can be seen in figure 2.1 where a flexible circuit is wrapped around a camera body.

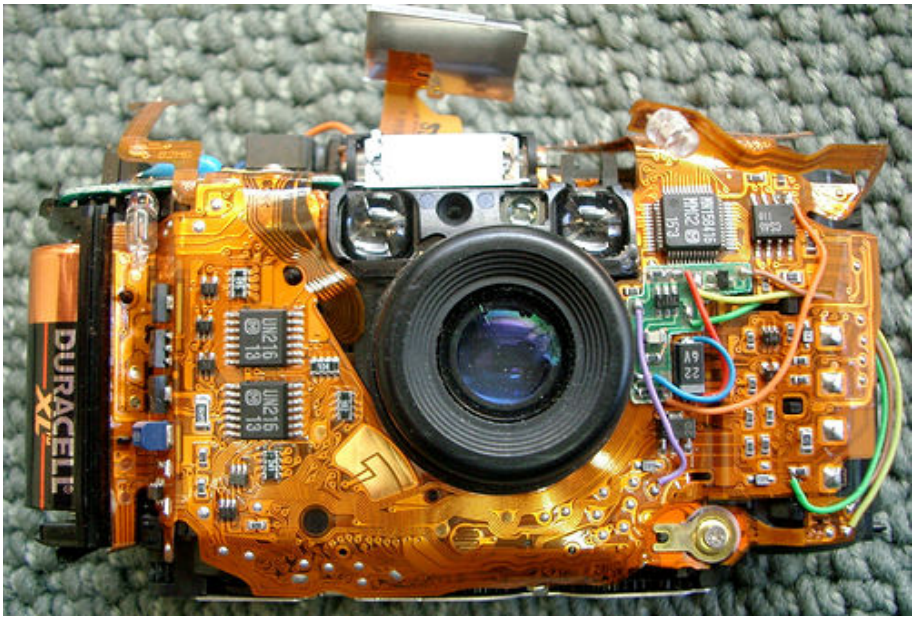

Figure 2.1: A flexible circuit in an Olympus Stylus camera. [8]

In a dynamic application the circuit is flexed during use. Flexibility can be utilized in circuits that go through hinges like those in laptops and foldable mobile phones. Many desktop printers also have flexible circuits which are used to connect moving parts. Dynamic applications especially place demands on the durability and reliability of interconnections and component joints in flexible circuits. [7]

Aside from flexibility, flexible printed circuits (FPC) have also other attractive qualities compared with rigid printed circuit boards. FPCs offer reduction in package size as the used substrates are usually much thinner than rigid substrates. Reducing package size also leads to reduction in package weight.

2.2 Common Flexible Circuit Manufacturing Processes

The manufacturing processes in the flexible circuit industry are many. Different process steps are used for producing single-sided, double-sided and multilayer circuits. In this section different processing options are discussed and the focus is on double-sided flex circuit manufacturing process. The idea is to give the reader a basis of a traditional manufacturing process to be compared later with a novel technology.

The basic elements of a flexible circuit are polymer film as the base material, possible bonding adhesive, metal foil and cover layer. A flexible base material and metal are joined to create a laminate, on which the circuit is the processed. Usually polyimide or polyester is used as the base material. Bonding adhesive is used to attach the metal layer to the base material. It is also possible to manufacture adhesiveless metal clad laminates by either casting the polymer direct on to a carrier foil or by depositing a seed layer of copper on a base film and building up the metal

layer by electroplating. While copper is mostly used, other metals can be used to satisfy special demands. A cover layer is used to protect the conductors of a flexible circuit. Cover layers can be e.g. laminated, photoimageable or screen-printed and cured by heat or UV-radiation.

2.2.1 Copper Processing Options

Due to copper's cost, good electrical performance and physical properties it is the most commonly used metal in flexible circuit metallic layers. Copper can be deposited on substrate by using various methods. Some of these methods and the grain orientations are presented in figure 2.2.

Electrodeposited copper is good for use in static applications, but due to the columnar grain structure it is not well suited for dynamic applications [7]. Wrought or rolled and annealed copper is produced by thinning copper with a series of metal rollers and then heat treating the metal foil. Commonly copper foils down to 18 μm thickness can be produced economically. Rolled and annealed copper is the most commonly used foil type in flexible circuit applications and due to the grain structure it is well suitable for dynamic applications [7]. Electroplated copper is deposited on a substrate by using a combination of electroless and electrolytic plating. Electroplated foils can be produced to have an amorphous grain structure.

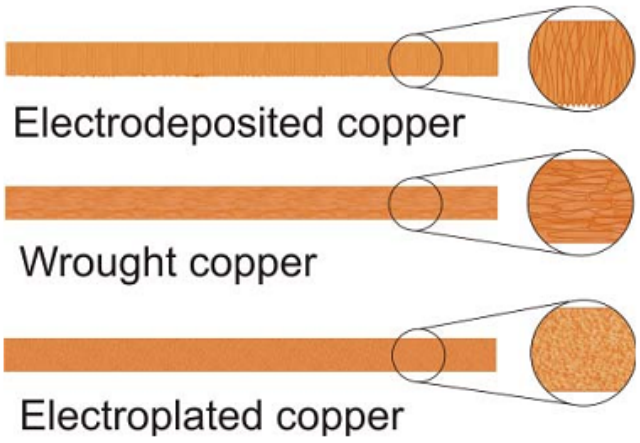

Figure 2.2: Different copper film production methods and grain structures. [7]

2.2.2 Flexible Circuit Types

There are several constructions of flexible circuits for several different applications. Depending on the complexity of the circuit design the flexible circuit can be manufactured to have one, two or several conductive layers by using different manufacturing processes. Most common types of flex circuits are shown in figure 2.3.

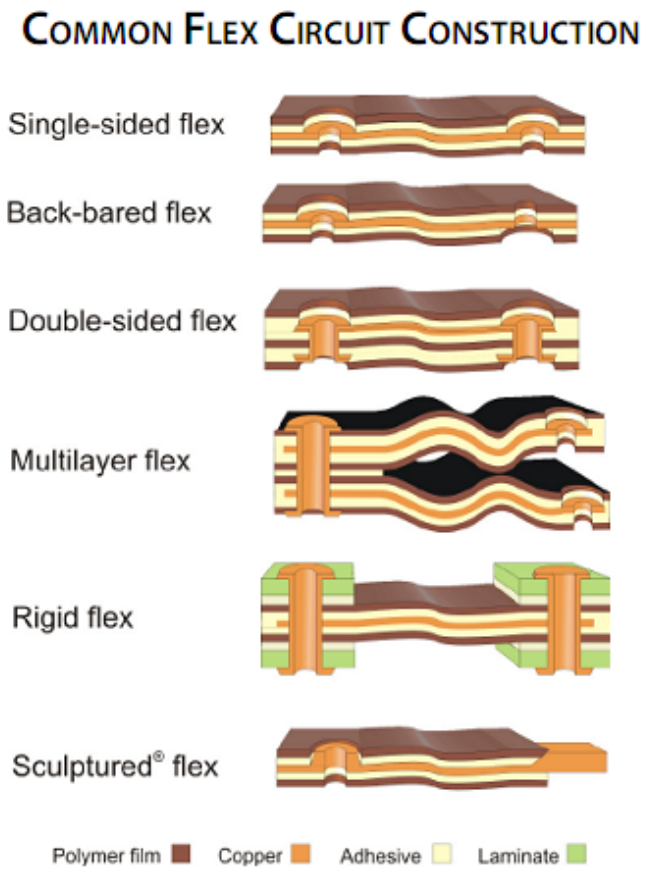

Figure 2.3: Basic flexible circuit constructions. [7]

The single-sided flex circuit is the simplest construction. A single-sided flex circuit consists of a conductor layer on a flexible base film and usually has a protective coating. Component connections can be made from one side only. A back-bared flexible circuit is a similar to the single-sided flex circuit, but the conductive layer is accessible from both sides, thus enabling component connections on both sides.

Double-sided flex circuits have two conductive layers on a flexible substrate. Usually double-sided flex circuits have plated through vias for connecting the conductive layers and component connections can be made on either side. Double-sided flex circuits can be manufactured with a protective layer on one, both or neither side.

Multilayer flex circuits have three or more conductive layers. Usually the conductive layers are connected by plated through vias. The layers of a multilayer flex circuit can be separately laminated in some regions of the circuit to enable routings to different areas or to enable maximum flexibility.

A rigid-flex circuit is a hybrid construction of a flexible and a rigid substrate that are connected together into a single structure. The electrical interconnections in the rigid and flexible interface are usually made by plated through vias. Rigid-flex circuits are usually multilayer constructions, but double-layer constructions also exist.

Sculptured flex circuits have conductors which vary in thickness in different places of the circuit. The usual goal is to make thin conductors in flexible places and thick conductors at interconnection locations. Selective etching of copper foil is used to attain different thicknesses of conductors in different areas of the circuit. [7]

2.2.3 Double-sided Flex Circuit Manufacture

A typical panel plating manufacturing process for double-sided flexible circuits is described in figure 2.4. The process starts with drilling or punching holes on a substrate. The substrate is plated with copper on either side. After the hole processing the holes are metalized using an electroless plating process or an alternative metallization process. After electroless metallization the copper layer in the holes is built up to sufficient thickness by electroplating.

After the plating of holes and the panel a resist image of the circuit pattern is applied on the both sides of the laminate. The exposed copper is then chemically etched and the remaining copper areas form the actual circuit. After etching the copper the remaining resist material needs to be stripped before applying the cover layer on top and bottom sides of the circuit board.

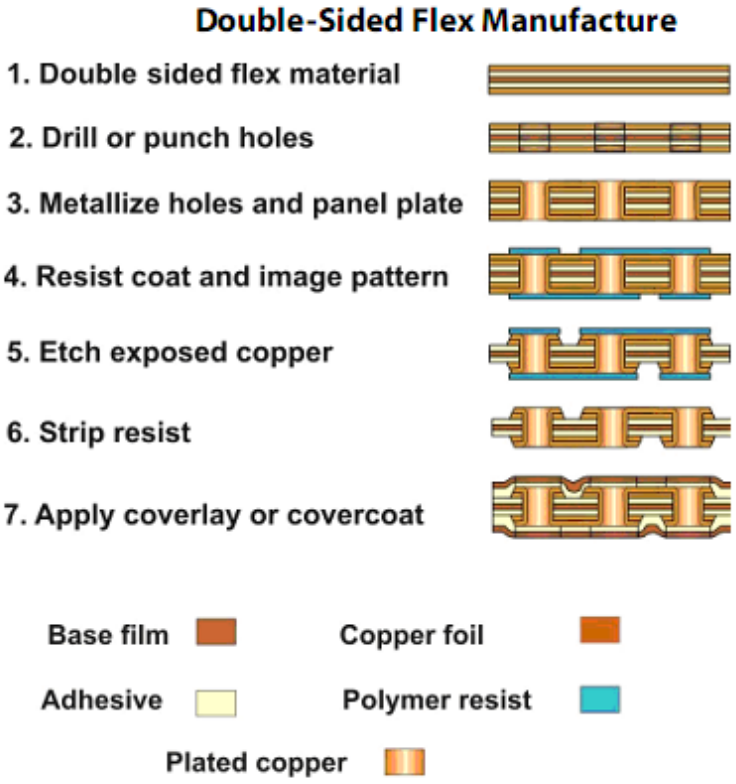

Figure 2.4: Double-sided flexible circuit manufacturing process [7].

2.3 Flexible Printed Electronics and Inkjet Technology

Many traditional printing methods are making their way to electronics manufacturing. For example, gravure printing, flexography and screen printing can be used for spreading conductive pastes, semiconductors and dielectrics on different substrates. Inkjet technology is one of the novel techniques being evaluated for the use of electronics manufacturing. Inkjet technology differs from the previously mentioned printing methods in some ways. The pattern file is stored in a digital format, rather than in a physical format on a plate or a roll. Digital pattern format enables easy and fast pattern redesign and also lowers the fixed costs in the beginning of the design process as there is no need for physical devices as gravure plates or flexographic printing plates. This is very beneficial in small volume manufacturing and prototyping. Inkjet technology is also a contactless technology. This means that the deposition tool, the print head, does not touch the substrate during deposition process. Patterning on rigid and flexible substrates is possible. Contactless deposition also enables processing on three dimensional substrates.

Manufacturing flex circuits by using inkjet-technology differs from common flex circuit manufacturing in several ways. Inkjet-printing is an additive process, where no excess material is deposited on the substrate while circuit processing. No premanufactured laminate of flexible polymer film and metal foil is needed before circuit processing as the circuit is inkjetted straight onto a polymer substrate. This way the material loss during circuit manufacturing is minimal. As conductors and dielectric layers can be processed without applying photoresist layers and etching chemicals, process steps are reduced and environmental load of the manufacturing process is small.

In this section the basic principles of producing electronic circuits using inkjet technology are presented. Emphasis is on making conductive circuits using inkjet technology, while other areas are may be covered with less attention. Inkjet printer operational principles are discussed along with nanoparticle ink properties.

2.3.1 Inkjet Printer Operational Principles

Inkjet printer deposition methods can be divided into continuous deposition and Drop-on-Demand deposition. Continuous deposition means that drops are deposited in a steady rate, needed or not, and are then deflected towards the substrate or collected to be used again. Drop-on-Demand means that a drop is fired from the nozzle plate only when it is intended to be deposited on a substrate. Simplified diagram of the operation of a piezo-controlled Drop-on-Demand inkjet is presented in figure 2.5. Ink is fed from the ink reservoir to the nozzles and a drop is formed by actuating the ink inside the nozzle cavity by a pulse. The actuating pulse can be

generated in several ways. Thermal, acoustic, electrostatic and piezoelectric pulse generation methods are used [9].

The printhead in figure 2.5 uses a piezoelectric element to actuate the ink inside nozzle cavities. An electrical pulse is given to the piezoelectric element and the transformation changes the volume inside the nozzle cavity. This volume change forces an ink drop out of the nozzle cavity towards the substrate. Drop formation can be controlled by changing the driving pulse's rise and fall times along with amplitude. Furthermore, the ink reservoir and the nozzle plate can be heated with a heater resistor to affect the viscosity of the ink to control drop formation. An image is formed by firing drops from the printhead while moving the printhead over a substrate or a substrate underneath the printhead in a steady speed.

Typically Drop-on-Demand printheads have multiple nozzles, typically ranging from around a hundred pieces to several hundreds. In the newest printheads the firing pulse can be individually adjusted to each nozzle for optimal performance.

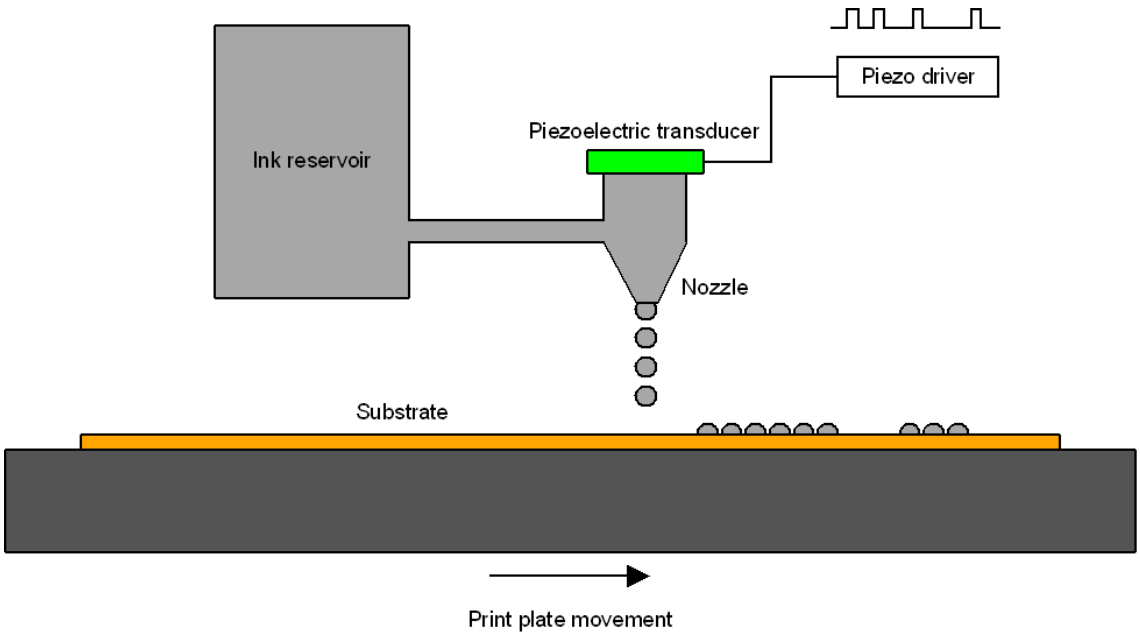

Figure 2.5: Operation of a piezo-guided Drop-on-Demand inkjet

In continuous inkjet deposition method drops are formed continuously by utilizing the tendency of a fluid stream to break up into small drops. Plateau-Rayleigh instability theorem describes that a fluid stream will break up to small drops if its length is ca. 3.13 to 3.18 times greater than its diameter [10]. Simplified diagram of the operation of a continuous inkjet is presented in figure 2.6. Ink is pumped from the reservoir to the nozzle plate and the ink is ejected from the nozzle by a piezoelectric transducer. After the fluid stream breaks into drops the selected drops are charged with a charging electrode. Statically charged field plates are used to deflect the charged drops from their original direction on to the substrate. The

dismissed drops are collected in a gutter and fed back to the ink reservoir. Image is created by moving the substrate under the printhead. [9]

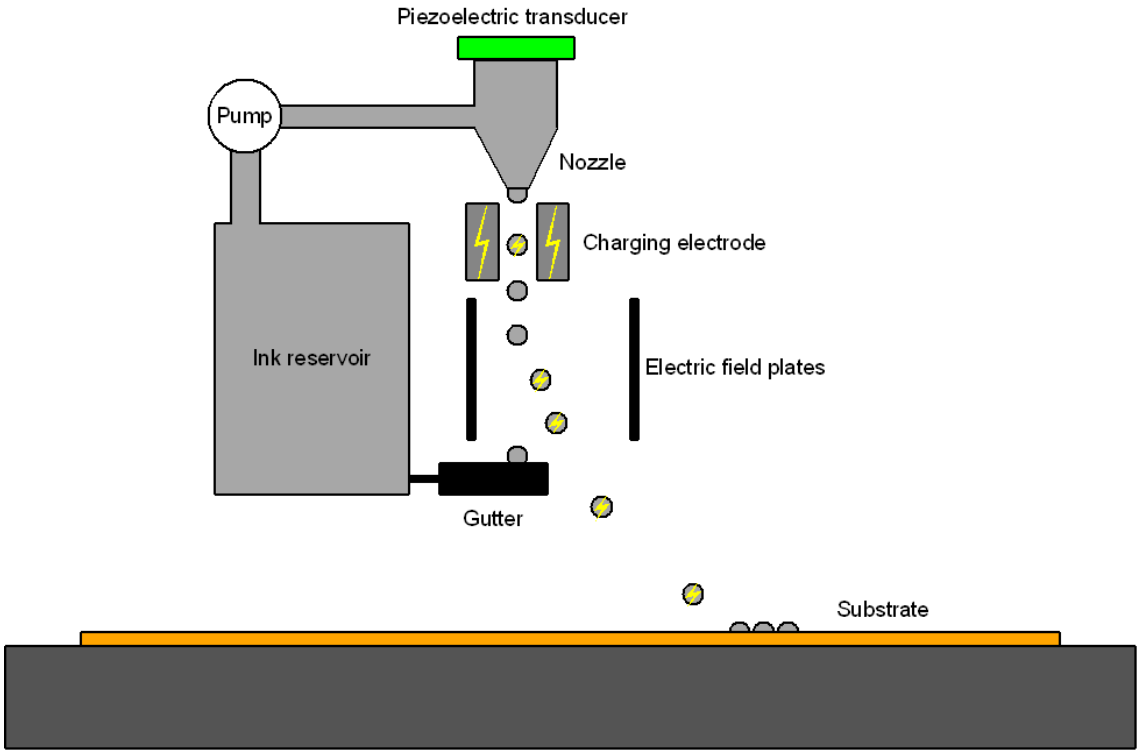

Figure 2.6: Operation of a piezo-guided continuous inkjet

Due to the discrete steps needed for drop formation in Drop-on-Demand inkjet printers, the firing frequency is lower than with continuous inkjet printers. Continuous inkjet is used for labeling purposes in food and medicine markets [9]. Continuous inkjetting has some demands which limit the possible use purposes and material possibilities. For example the used ink has to be conductive so that it can be charged and deflected. Drop-on-Demand inkjet does not place any demands on the ink conductivity, hence dielectrics can be printed. This matter along with multiple nozzle deposition possibility, ease of use and maintenance favor the use of Drop-on-Demand as a method for electronics manufacturing. [9]

2.3.2 Inks in Inkjet Technology

A wide range of inks can be printed using inkjet printers. Metallic nanoparticle inks are used to create conductive traces and dielectric inks are used to separate conductive layers or to create a covercoat for the printed structure. Also few semiconductor inks are available. Metallic nanoparticle inks are solvent-based or water-based and are cured by a thermal or photonic process, such as laser. Dielectric inks are usually UV curable. The product range of nanoparticle inks is wide. Silver and gold nanoparticle inks were one of the first inks to be developed. Cost related issues drive

ink manufacturers to develop new inks from cheaper bulk metals, such as copper. Also aluminium and nickel inks have been developed.

2.3.3 Nanoparticle Inks

Nanoparticle inks are the basis of making electronic circuits using inkjet technology. Nanoparticle inks usually consist of dispersant clad metal nanoparticles in solvent. Nanoparticles are covered with a dispersant to prevent the particles from clustering and to prevent oxidation. Due to the nanoscale size of metal particles, high metal content in a low viscosity fluid and low sintering temperature [11] can be attained. Issues related to ink jettability and wetting need to be considered while making the material selection and during the design phase of the inkjetted circuit. In the following two sections the importance of jettability and wetting are discussed briefly.

2.3.4 Nanoparticle Ink Jettability

Ink formulation is very important considering the jettability of the ink. The ejection of a droplet from a nozzle and drop formation is a complicated process affected by many factors. Interaction of the printing equipment and ink qualities determine how well the ink can be jetted from the printhead. The jettability of the ink can be predicted if the properties of the ink and the printing equipment are known. Reynolds number (see equation 2.1) describes the ratio of dynamic pressure to shearing stress and Weber number (see equation 2.2) describes the ratio of inertial forces to surface tension forces [12] [13]. In practice Reynolds number can be used to determine whether a liquid flow is laminar or turbulent e.g. in a pipe. When the Reynolds number is high the inertial forces dominate and the liquid flow is turbulent. On low Reynolds number values viscous forces dominate and the flow is laminar. Weber number is used for analyzing drop formation. Reynolds and Weber numbers can be presented by the following formulae

$$Re = \frac{va\rho}{\eta} \tag{2.1}$$

$$We = \frac{va^2\rho}{\gamma} \tag{2.2}$$

where v is the average drop velocity, a radius of the printing nozzle and ρ, η and γ are the density, viscosity and surface tension of the ink. A dimensionless number, the Ohnesorge number (O_h) is derived from Reynolds number and Weber number. The Ohnesorge number (see equation 2.3) is calculated by dividing the square root of Weber number by Reynolds number.

$$O_h = \frac{\sqrt{We}}{Re} \tag{2.3}$$

The inverse (Z, see equation 2.4) of the Ohnesorge number is used to determine the jettability of an ink theoretically. As can be seen, velocity has been reduced from the equation. Ink qualities and nozzle aperture size remain in the equation. [9]

$$Z = \frac{Re}{\sqrt{We}} = \frac{\sqrt{a\rho\gamma}}{\eta} \tag{2.4}$$

Depending on the source, different recommendations for the value range of Z for jettable inks are given. For example Fromm recommends the a value larger than 2 [14] and Jang et al. recommend a value from 4 to 14 [15]. The differences for recommendations come from differing methods and criteria used to determine the jettability of a fluid. In general, the Ohnesorge number is a tool for estimating the jettability and printing parameters of an ink theoretically. In practice, jettability and printing parameters should be determined by a dropwatcher device by studying the drop ejection and formation by a slow motion camera.

2.3.5 Nanoparticle Ink Wetting

The interaction of substrate and ink is a big part of inkjet printed circuit quality. With suitable materials ink spreading and wetting can be carefully controlled to enable optimal print quality. On the other hand, poor matching of ink and the substrate results in reduced print quality. The most important factors that affect ink wetting on a single drop deposition scale are ink qualities, such as viscosity, surface tension and density, substrate qualities, such as surface roughness and surface energy along with substrate temperature. On a larger scale, when multiple drops are deposited simultaneously, ink wetting becomes more complex. Drop deposition sequence, printing speed and the geometry of the printed pattern affect the quality of the print. In this section the substrate-fluid interaction is studied mostly on single drop deposition scale. The effect of drop placement sequence and printing speed will be discussed later.

The drop impact on the substrate can be divided into three phases: impact-driven phase, relaxation-oscillation and capillary driven phase [16]. Examples of evolution of the drop shape can be seen in figure 2.7. The impact-driven phase is very brief, typically lasting few tens of microseconds. The impact phase is mainly dictated by the inertia of the drop. After the impact phase there may be oscillation in the droplet diameter, depending on the ink and substrate qualities and the remaining inertia of the droplet. The oscillation eventually dampens and the capillary driven phase

takes place. The events taking place during the capillary driven phase are quite complex and depend largely on the ink, substrate and environmental qualities. To put it simply, during the capillary driven phase the inertia of the droplet has reduced to a negligible amount and the spreading is driven by material and environmental properties. The drop spreads until its reaches equilibrium state. [9] [16]

Other than modifying the ink formulation, spreading can be controlled by modifying the surface energy of the substrate and by heating the substrate. The substrate can be chemically treated with an anti-wetting agent to prevent excess spreading of the ink when printing fine structures. Alternatively a pro-wetting coating can be applied if good wetting is needed. Heating of substrate increases the evaporation rate of solvent from the drop, thus affecting the viscosity of the ink drop. Concerning metallic nanoparticle inks, this slows down the spreading in capillary driven phase, as the drop turns solid rapidly.

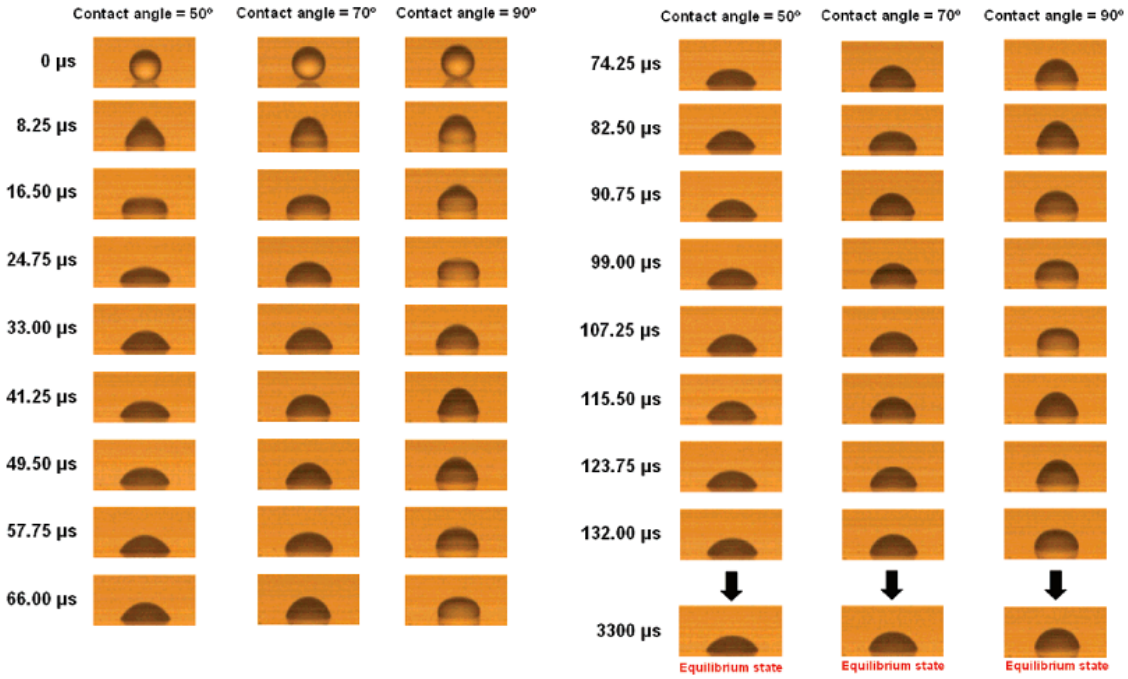

Figure 2.7: Examples of drop behaviour upon impact. [17]

2.3.6 Sintering

In sintering phase the ink deposited on a substrate becomes conductive. The dispersion agent is removed from the surface of the nanoparticles and the particles merge together to form a conductive structure. The most common method for sintering is heat transfer by a convection oven [18] [19]. Recently available copper nanoparticle inks require photonic sintering, e.g. laser [20], to speed up the sintering process to avoid particle oxidation.

Overview of the ink drying and sintering process is presented in figure 2.8. As ink is deposited on the substrate the solvent evaporation begins. Most of the solvent is usually evaporated during printing, depending on the substrate temperature. When the printed structure is transferred to an oven, the remaining solvent evaporates. When enough heat is transferred to the structure the dispersant is removed from around the nanoparticles and the particles merge together.

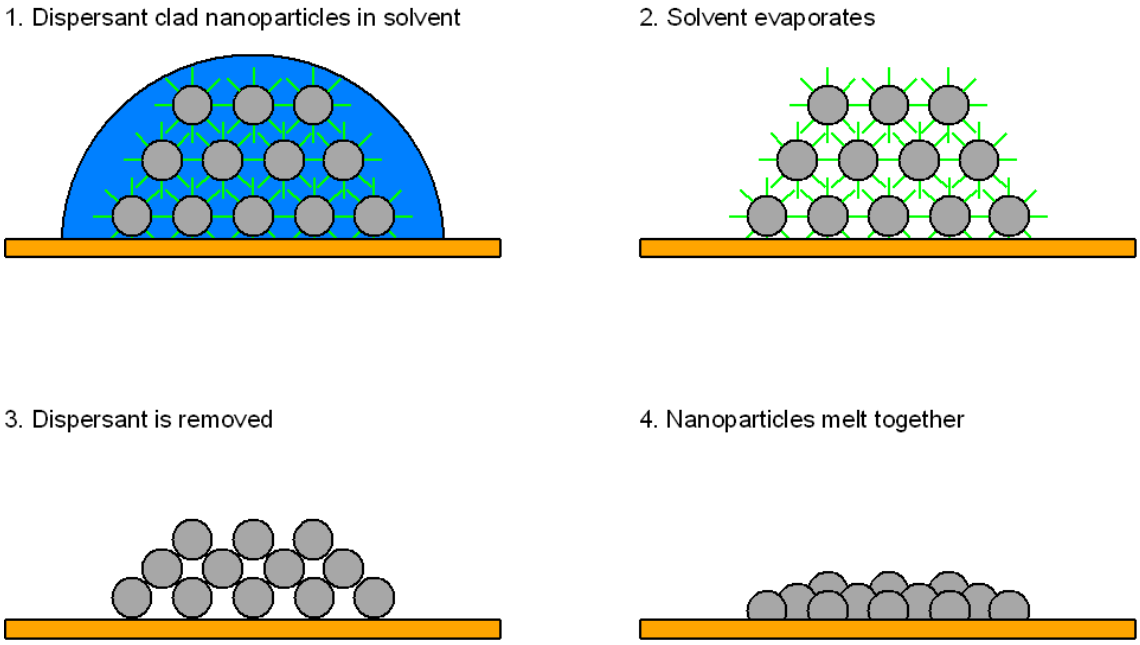

Figure 2.8: A simplified overview of the ink drying and sintering process.

Harima NPS-J silver nanoparticle ink was used in this thesis work. The properties of this ink will be discussed later. The sintering time instructed by the supplier for Harima NPS-J silver ink is 1 hour in 220 °C. The sintering of NPS-J silver nanoparticle ink as a function of time can be seen in figure 2.9. A drastic drop in resistance can be seen within the first 20 minutes of the sintering. After that the resistance stabilizes. The drop in resistance at 1 hour mark is due to sample removal from the convection oven. The resulting sheet resistance is ca. 0.040 Ω/□. A small knee can be seen right before the stabilization of resistance at about 15 minutes from the beginning of the sintering. The reason for the knee is not certain, but it is suspected to be the point where the dispersion agent is removed from around the nanoparticles and the particles melt together [21].

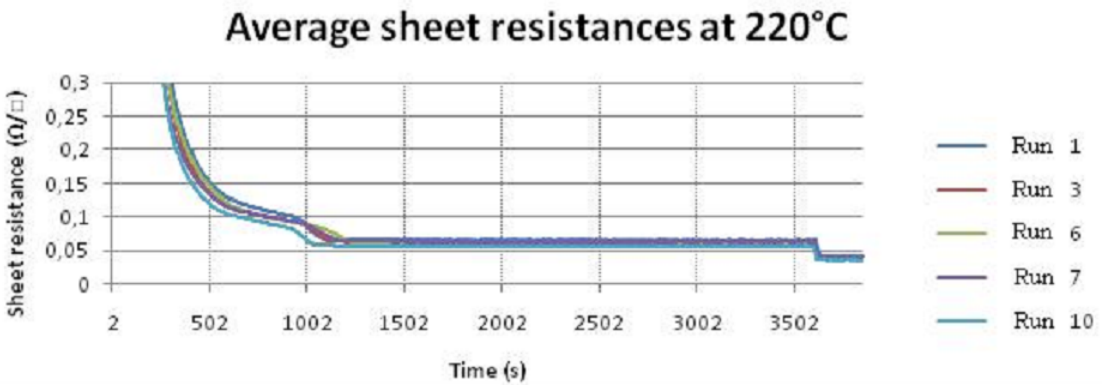

Figure 2.9: Square resistance of NPS-J silver nanoparticle ink as a function of time. Resistances were measured during sintering from 5 cm long, 300 μ m wide lines, which were placed in a convection oven. Horizontal axis is time in seconds, Vertical axis is the square resistance of the samples. [21]

3. DEVICE DESIGN CONVERSION TO INKJET TECHNOLOGY

A flexible printed circuit board (PCB) of a mobile phone was decided to be manufactured with inkjet printing technology as a technology demonstrator. The original product design was modified due to the change of manufacturing technology. New materials were selected and the original design files were modified the iTi inkjet printer for PCB manufacturing and for the Corelase X-LASE laser for via drilling. In this chapter the flex-module properties are presented and the material selection and the design modifications are discussed. The idea is to explain the design considerations from the point of view of inkjet technology.

3.1 Device Description

In this section the features of the flexible PCB module are introduced. Demands placed by the original design are discussed and viewed from the point of view of printable electronics.

A flexible PCB was selected as a demonstrator device to be manufactured by the means of printable electronics. The selected flexible PCB is a part of a basic mobile phone. The mobile phone has a sliding mechanism and a flexible PCB is needed to connect the display, keyboard and earpiece to the main PCB of the phone. The display, earpiece and keyboard are located on the slider bar and the flexible PCB is needed to make the connection between the moving slider and the motherboard. Connection is made through holes in the slider frame and the motherboard. The flex-module and the slider mechanism can be seen in figure 3.1.

The flexible PCB has two connectors, two stiffener plates beneath the connector areas, a keyboard and some passive SMT components which include LEDs for illuminating the keyboard. The functional parts of the flex-module and their interfaces to the actual PCB are described in figure 3.2.

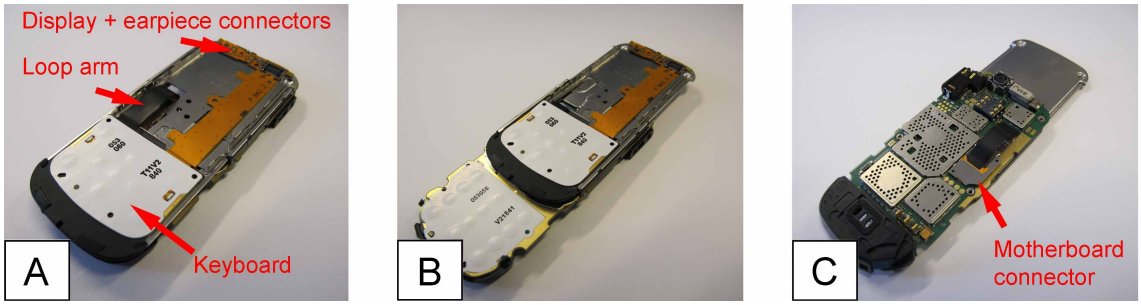

Figure 3.1: Flex-module, sliding mechanism and the motherboard of the mobile phone. On the left side figure (A) the sliding mechanism is closed and on the middle image (B) the sliding mechanism is open. On the rightmost image (C) the connection of the flex-module and the motherboard can be seen.

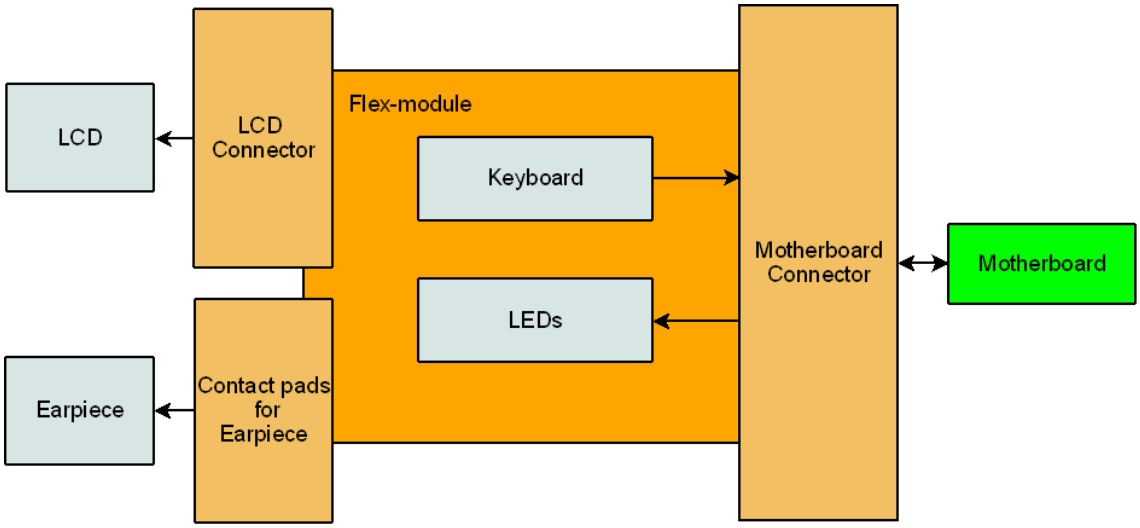

Figure 3.2: Interface diagram of the flex-module. The brown boxes represent the connectors and connection pads of the flex-module. The blue boxes represent the main functional parts connected to the flexible PCB. The green box represents the motherboard. Arrows point out the direction in which data is transmitted.

3.1.1 Display and LEDs

The flexible PCB connects the LCD display to the motherboard of the mobile phone. The display is connected to the motherboard with 13 data lines, including write line, reset line, data/command select line, read line and eight data lines. There are also routings for grounding and supply voltages. The smallest line widths and gaps used in the display control lines in the original design are 75 μm wide. The control lines run in an u-shaped curve between the two connectors in the flex module (see figure 3.3). The approximate length of the traces is about 12 cm. The manufacturing and performance of the display control lines was expected to be one of the challenges when transferring the design to inkjet technology, as the resistance of the lines was expected to rise compared to the original design. The performance of the inkjetted

display control lines was tested and will be discussed later in the testing chapter.

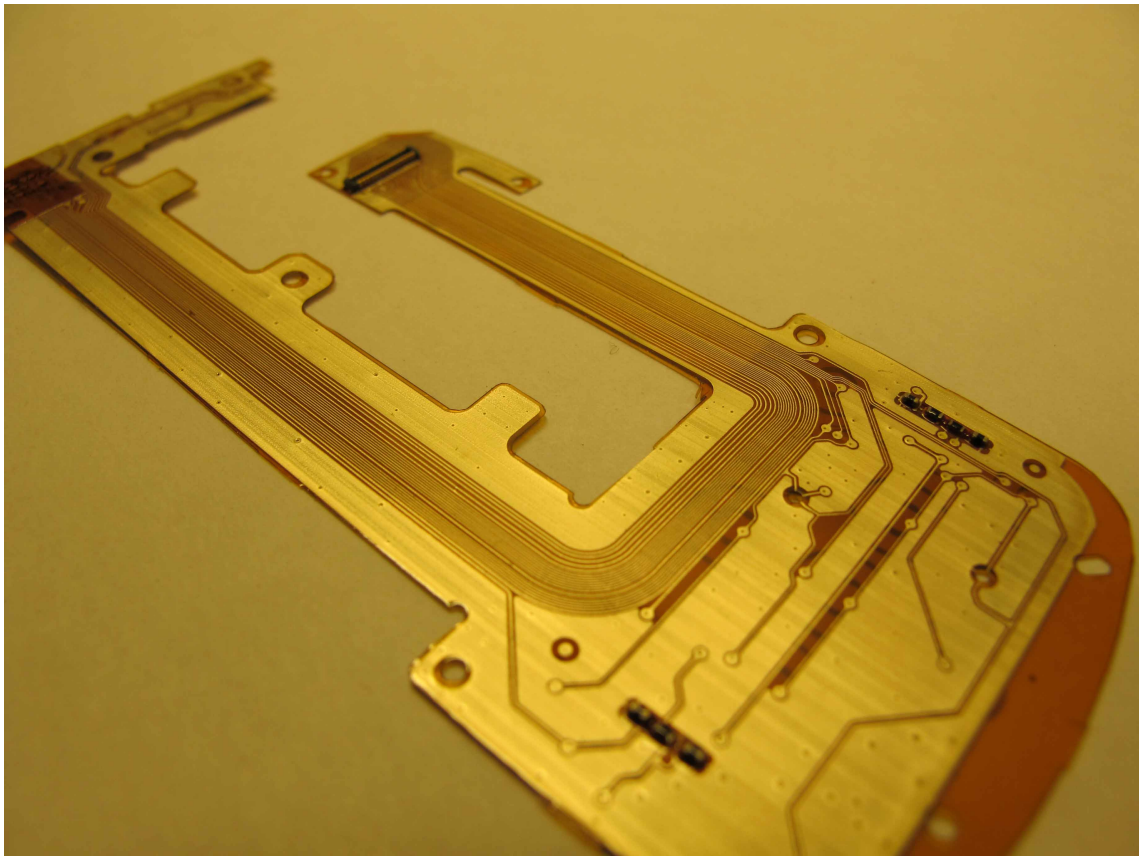

Figure 3.3: Display control line routings on the flex module.

The flexible PCB has two LEDs for illuminating the keyboard. LEDs are placed on the top layer of the board and on the opposing side there are resistors and varistors. The resistors are used as ballast resistors for the LEDs and varistors are used for controlling the light-up time and dimming time of the LEDs.

3.1.2 Keyboard

This mobile phone has two keyboards. The keyboard on the flex-module is used for answering calls, ending calls and moving around in the menu. The power-on-key is also on this keyboard. The other keyboard is on the motherboard and it is used for the input of numbers and characters. The keyboard in the flex-module has nine keys. The keyboard is constructed by placing an adhesive sheet with metallic domes on top of the printed circuit board. The dome is pressed against the circuit board to create a galvanic contact between separated areas. Data from the keyboard is transmitted to the motherboard by seven data lines which include two lines for reading rows, six lines for reading columns and one line for the power-on-key. The keyboard construction can be seen in figure 3.4.

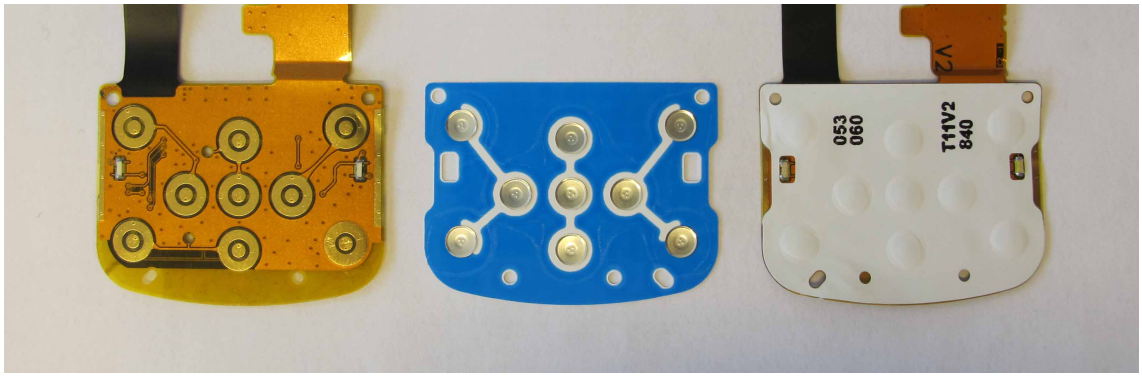

Figure 3.4: Dome keyboard of the flexmodule.

One design concern at the beginning of the project was the endurance of inkjetted keyboard pads. The concern was if the mechanical stress caused by the metallic domes would wear out the inkjetted layer as the inkjetted conductive layer is only a few micrometers thick. When the metallic dome is pressed it connects the separate pads. During this transformation minor friction is inflicted on the outer rim of the dome. On a standard PCB this is not a problem as the metallic is much thicker than an inkjetted metallic layer. However, it was unclear if an inkjetted metallic layer would withstand this kind of long term mechanical stress. Now it can be said that during the testing phase no defects caused by mechanical stress of the keydomes were observed, though the long term effects remain unknown.

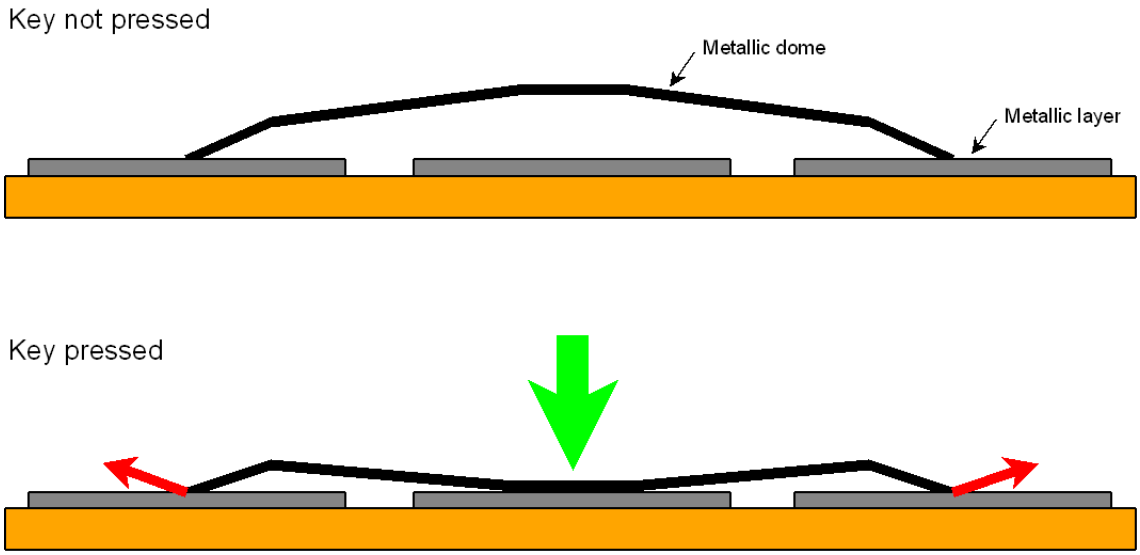

Figure 3.5: Mechanical stress caused by the dome movement.

3.1.3 Earpiece

The flexible PCB also connects the earpiece component to the motherboard. The earpiece component is connected to the PCB by a plastic holder which pushes the component against the PCB surface. There are four connection pads on the component to be connected to the PCB and one pad for grounding the component in the metal slider. Two signal lines are directed from the motherboard through the flexible PCB to the earpiece component. There are filtering components on the flexible PCB for the removal of noise from the signal lines.

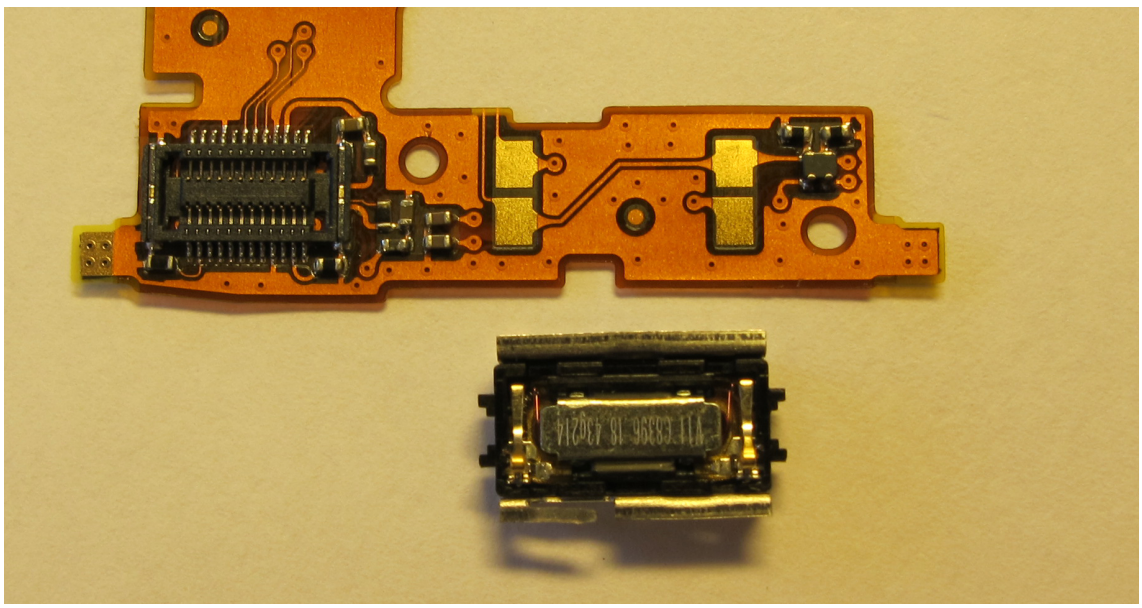

Figure 3.6: Earpiece connector pads and the earpiece component.

3.2 Material Selection

One of the first steps of the design phase of the inkjetted flexible PCB prototype was the material selection. Overview of the material selection can be seen in table 3.1. The substrate material and nanoparticle ink were selected at the start of the project. Other materials were selected during the design and manufacturing of the first inkjetted prototypes. The cheapest possible materials were not selected yet for prototyping. It was decided that the building of the inkjetted prototype was first to be carried out with familiar materials.

Purpose	Material
PCB interconnections	Harima NPS-J silver nanoparticle ink
Substrate material	Kapton polyimide film
Component attachment (electrical)	Creative 124-08C
Component attachment (mechanical)	Epotek U-300 underfill epoxy
Conformal coating	Hysol PC28 STD Spray-on varnish
Striffener plate material	Kapton polyimide film

Table 3.1: Material selection of the inkjetted flexible PCB prototype.

The selected conductive nanoparticle ink was Harima NPS-J. Harima NPS-J material properties can be seen in table 3.2. Harima NPS-J ink was selected because of its good performance and reliable jetting (Harima NPS-J has a Z value of 2.68 [12]).

NPS-J properties	
Particle Size	8-15 nm
Metal Content	62-67 wt%
Solvent	Tetradecane
Viscosity	7-11 mPa·s
Specific Gravity	1.8-2.2
Sintering	220 °C (60 min.)
Specific Resistance	3$\mu\Omega\cdot$ cm
Thickness Shrinkage	80-85 %

Table 3.2: NPS-J properties. [22]

The selected substrate material was Kapton HN-200 polyimide film. It was selected because it has been previously used when making inkjetted applications with Harima NPS-J ink. The main reason for the use of Kapton polyimide film is the high sintering temperature of Harima NPS-J ink. Kapton has a good heat stability and it can withstand temperatures up to 400 °C. The selected film thickness was 50μm. Some properties of Kapton HN film are listed in table 3.3.

The component joints to the PCB were made by solder in the original design.

Kapton HN-200 properties	
Usable Temperature Range	−269 °C - 400 °C
Melting Point	None
Thermal Coefficient of Linear Expansion	20 ppm/ °C
Shrinkage (30 min at 150 °C)	0.17%
Dielectric Constant	3.4 (1 kHz)

Table 3.3: Kapton HN-200 properties. [23]

Isotropically conductive adhesive was used in the inkjetted version due to the incompatibility of inkjetted circuits and soldering [24]. The selected ICA was Creative Materials 124-08C. 124-08C is a syringe dispensable, heat cured, flexible, silver-filled epoxy adhesive. This ICA was selected because of its relatively fast heat curing time and flexibility. 124-08C material properties can bee seen in table 3.4.

Creative Materials 124-08C properties	
Volume Resistivity	0.0002 to 0.0004 Ω·cm
Thermal Conductivity	6.5 W/mK
Glass Transition Temperature (Tg)	120 °C
CTE below Tg	$33 * 10^{-6}$ in/in/°C
CTE above Tg	$84 * 10^{-6}$ in/in/°C
Tensile Shear Strength	1500 psi
Specific Gravity	2.6
Useful Temperature Range	−55 °C to 200 °C
Thermal Stability	Good to 300 °C

Table 3.4: Creative Materials 124-08C ICA properties. [25]

ICA joints have a fairly poor mechanical strenght compared to solder joints. A flexible PCB places high demands on the strenght and quality of the component joints. The mechanical strength ICA component joints to the PCB was enhanced by surrounding the ICA attached components with underfill epoxy material. The selected epoxy material was Epotek U300. Material properties of the used underfill material can be seen in table 3.5.

Epotek U300 properties	
Volume Resistivity	0.0002 to 0.0004 Ω·cm
Thermal Conductivity	6.5 W/mK
Glass Transition Temperature (Tg)	120 °C
CTE below Tg	$33 * 10^{-6}$ in/in/°C
CTE above Tg	$84 * 10^{-6}$ in/in/°C
Tensile Shear Strength	1500 psi
Specific Gravity	2.6
Useful Temperature Range	−55 °C to 200 °C
Thermal Stability	Good to 300 °C

Table 3.5: Epotek U300 Underfill Material properties. [26]

3.3 PCB Layout from Gerber to Bitmap

The original design files from the manufacturer were given in Gerber format. The received files included top and bottom side PCB layouts along with via drill files and component placement files. The top and bottom PCB layout files were modified for the iTi inkjet printer. Files were converted from Gerber format to TIFF format and modifications were made to the converted TIFF files. Overall description of the circuit layout files conversion process is presented in figure 3.7.

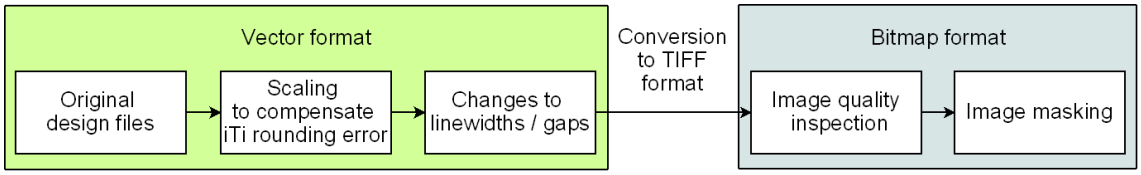

Figure 3.7: PCB layout conversion process.

3.3.1 Changes to Original PCB Layout

The iTi inkjet printer uses TIFF images as input files. The printed file is selected in the iTi inkjet printer XY-stage control software and the file resolution is selected in process (print plate x-axis) and cross-process (print plate y-axis) direction. The resolution in the cross-process direction can be selected from 50 dpi to 5050 dpi with 50 dpi increments. The resolution selection in process direction can be freely selected but after setting of resolution the control software rounds the selected resolution to a suitable resolution for the hardware. The rounding is done because imperial units system is used to control the hardware. When a 5050 dpi resolution is selected in process direction iTi control software rounds the number to 4884.615 dpi. This means that the printed pixel is bit longer in process direction than in cross-process direction. The pixel width in process direction is the length of one inch divided by

the resolution in process direction, i.e. amount of pixels per one inch (see equation 3.1).

$$\frac{0.0254 \text{ m}}{4884.615} = 5.20 \ \mu\text{m} \tag{3.1}$$

And in cross-process direction the pixel height is the length of one inch divided by the resolution in cross-process direction, i.e. amount of pixels per one inch (see equation 3.2).

$$\frac{0.0254 \text{ m}}{5050} = 5.03 \ \mu\text{m} \tag{3.2}$$

The error in the pixel process dimension is the intended pixel width substracted from the actual width (see equation 3.3).

$$5.20 \ \mu\text{m} - 5.03 \ \mu\text{m} = 0.17 \ \mu\text{m} \tag{3.3}$$

In high resolutions as in 5050 dpi this error accumulates to a significant amount. The generated TIFF image had 16986 pixels in process direction and 7800 pixels in cross-process direction. With 0.17 μm error in the processing direction per pixel, the total error in the image can be calculated by multiplying the error per pixel by the amount of pixels in the image process direction (see equation 3.4).

$$16986 \text{ pixels} \times 0.17 \frac{\mu\text{m}}{\text{pixel}} = 2.9 \text{ mm} \tag{3.4}$$

To compensate the rounding error in iTi printer the original Gerber files were scaled shorter in process direction before conversion to bitmap images so that with the XY-stage control software's rounding error the image would realize to be in the original dimensions. The scaling factor can be calculated by dividing the resolution given by iTi's software with the intended resolution (see equation 3.5).

$$\frac{4884.615 \text{ dpi}}{5050 \text{ dpi}} = 0.967 \tag{3.5}$$

After the scaling in process direction the line widths were trimmed so that the line widths in the inkjetted design would result in about same line widths as in the etched version of the circuit. The actual inkjetted lines are wider than on the bitmap file because the drops on a substrate have a larger diameter than the size of pixels in a bitmap file. For this reason the interconnection lines in the Gerber layout file were made thinner.

The line widths in the Gerber-file were redefined by using equation 3.6. The symbols and origin of equation 3.6 are explained in figure 3.8. The basic parameters needed for the estimate are inkjetted drop diameter (d), pixel size in the used bitmap resolution (W_{pixel}) and the desired line width (W). The line widths in the Gerber file

(W_{design}) need to be set so, that when the Gerber file is converted to bitmap-form, the traces will have the desired amount of pixels widthwise. This estimate is best applicable when the printed drops remain separate after printing i.e. in a stacked coin-like structure. The estimate can be used for more uniform lines also, but one needs to be sure that no over wetting is taking place during printing.

$$W_{design} = W - d + W_{pixel} \tag{3.6}$$

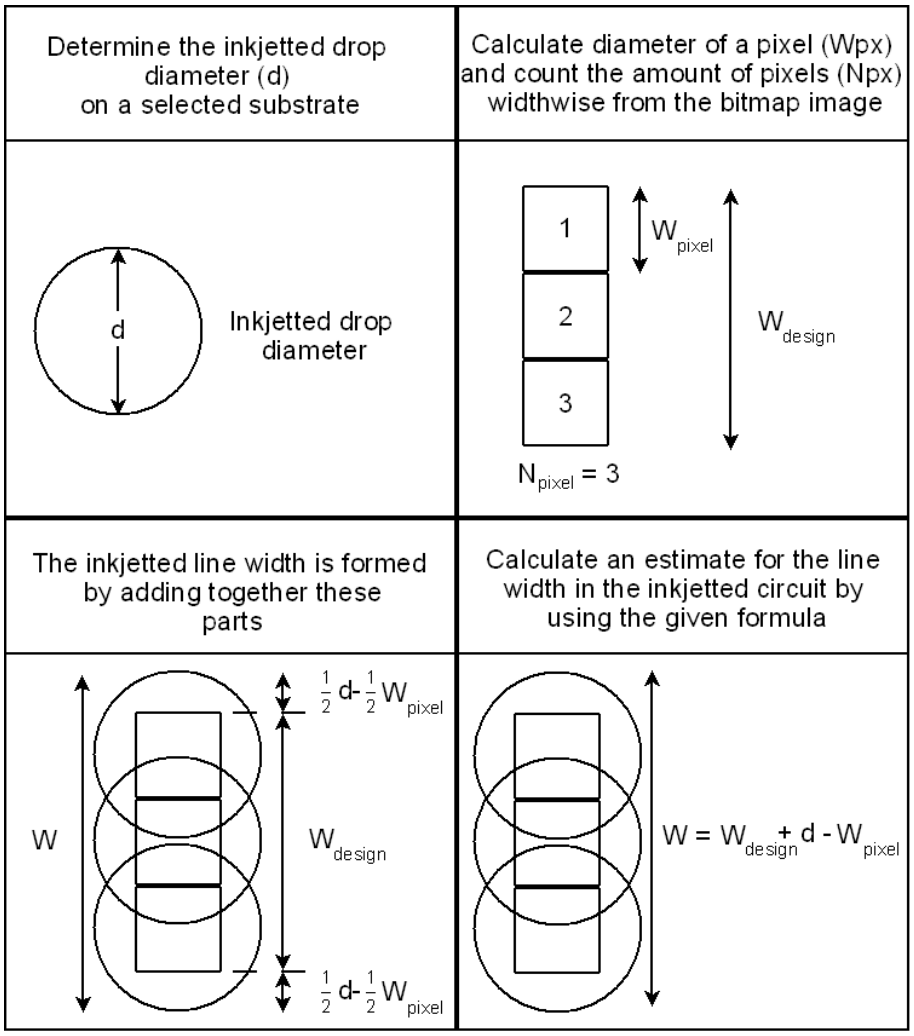

Figure 3.8: Method for estimating line widths in a layout design file. A three pixel wide line is used as an example.

3.3.2 Background for Bitmap Masking Algorithm

Inkjet technology places special demands on the design phase. Some of these issues, e.g. line widths, can be taken into account when designing the circuit in vector format, as discussed in the previous section. Some phenomena related to inkjetting need to be taken into account after transferring the circuit design into bitmap format. In this section these phenomena are pointed out along with the introduction of an image masking algorithm which aims to take these phenomena into consideration. Methods for controlling drop placement accuracy, deposited ink amount and drop placement sequence by modifying the bitmap image are introduced.

Image file resolution determines how accurately drops are placed on the substrate. The most accurate resolution with iTi XY 2.0 printer is 5050 dpi and this resolution was used when printing the layout. High resolution was chosen because of the high precision needed for drop placement. A smaller resolution would be sufficient from ink quantity point of view, but it would place restrictions on drop placement accuracy. For example, in 800 dpi resolution the drop spacing would be ca. 32 μm. This would cause significant placing error in a design file where the smallest line widths and gaps are around 75 μm. At 5050 dpi the spacing of adjacent drops is about 5 μm. This means that the position of an individual drop can be determined with 5 μm accuracy on the substrate. However, with 5050 dpi the drop spacing is very small compared to the drop size on substrate. Without any surface treatment a Harima NPS-J drop on Kapton Polyimide is about 90 μm in diameter when the print plate is heated to 70 °C and a Spectra SQ jetting assembly is used. While high accuracy can be achieved using 5050 dpi the short drop spacing causes line bulging or flooding easily. Flooding and bulging phenomena are related to the amount of ink deposited on the substrate per area, i.e. drop density, and the time delay between the deposition of adjacent drops.

Another challenge related to achieving good print quality is related to drop placement, i.e., the way in which the printhead deposits the drops on a substrate. Due to the operation of the printer the adjacent drops are deposited differently in cross-process and process direction. The time interval between adjacent drop deposition in process direction and cross-process direction is not the same. This easily leads to non-uniform print quality. To understand the problem one needs to understand the operation of the printerhead during printing (see figure 3.9). The printplate moves underneath the printhead in process direction and the printhead deposits drops on surface. After one sweep the plate moves back and makes a microstep for the next row of pixels to be printed during the next sweep. This sequence is carried out several times until the print plate has moved the length of the nozzle spacing in cross-process direction. Due to the operation the time interval between

adjacent drops deposited in process direction (Δt_1 in figure 3.9) is usually around few hundred microseconds and few seconds in cross-process direction (Δt_2 in figure 3.9).

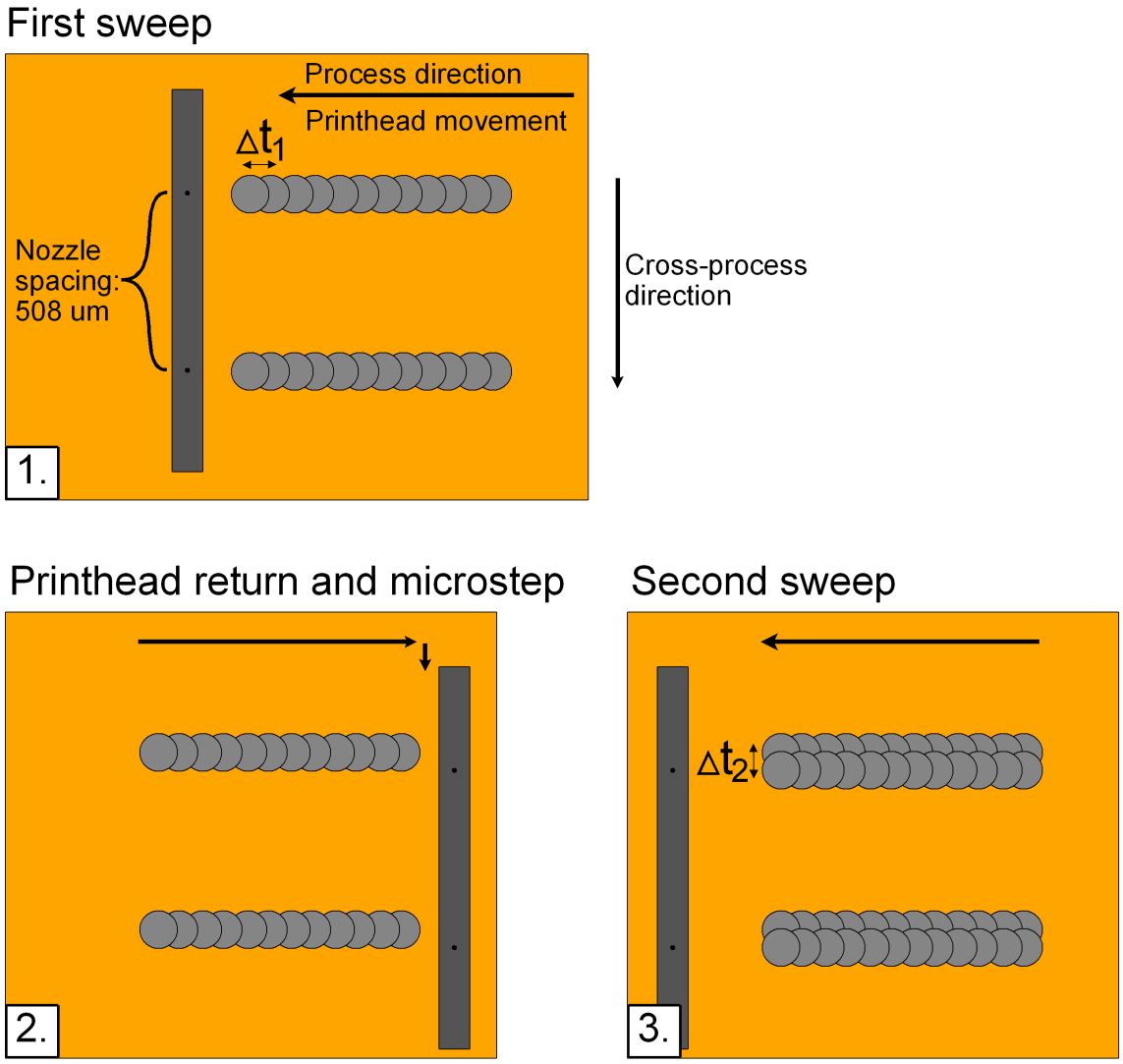

Figure 3.9: Printhead operation during printing. Δt_1 is the time interval between two adjacent drops deposited in process direction. Δt_2 is the time interval between two adjacent drops deposited in cross-process direction.

Example of non-uniform print quality is given in figure 3.10. The picture is taken from one of the early printing trials made with the flex module layout. Adjacent drops in process direction are formed as one continuous line unlike in the curve, where drops on different rows can be seen separately. The line formed by adjacent drops in process direction is uniform but it is also wider than in the curve where drops remain separate.

The problem with making uniform lines is to control the drop deposition so that the solvent has sufficient time to evaporate. Drop deposition delay, drop spacing and substrate temperature affect the inkjet-printed structure formation. If adjacent

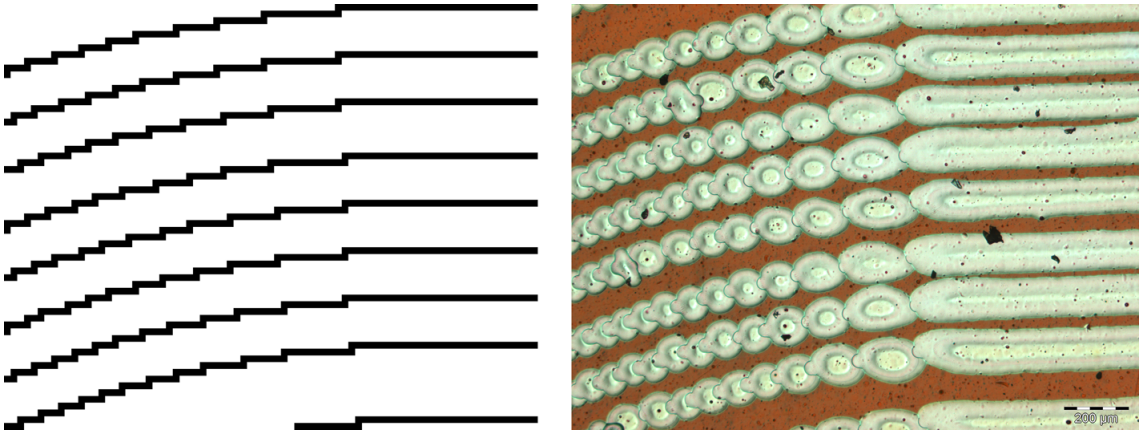

Figure 3.10: Example of poor, non-uniform print quality. 1200dpi bitmap image file on the left.

drops are deposited too close to each other or in a too fast rate, bulging or flooding will occur. The relation between drop deposition delay, drop spacing and printed structure morphologies is roughly explained in figure 3.11. As previously stated, the delay between adjacent drop deposition on process direction and cross-process direction is not the same. This places challenges on forming uniform lines in process direction and cross-process direction.

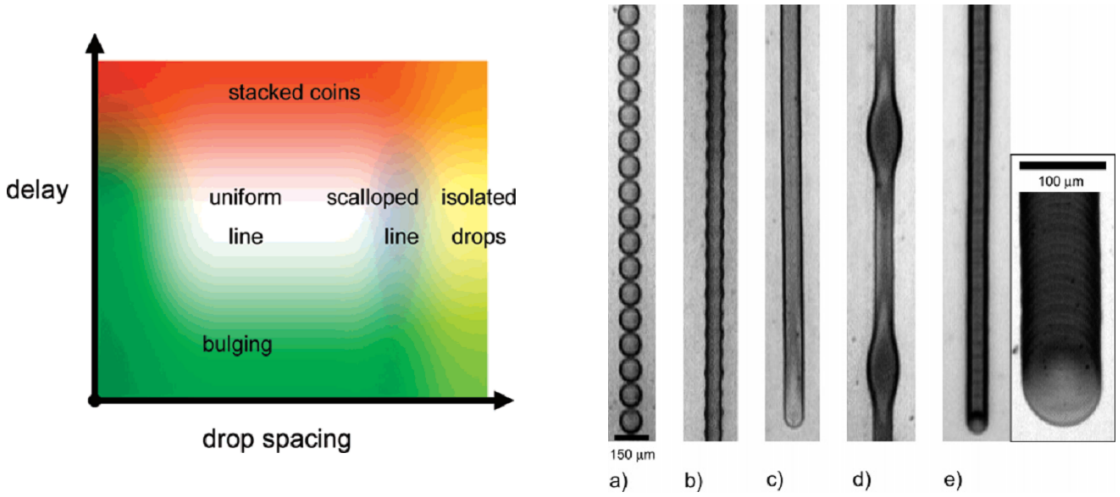

Figure 3.11: Relation between drop delay, drop spacing and structure formation. a) isolated drops, b) scalloped line, c) uniform line, d) bulging, e) stacked coins. [27]

3.3.3 Bitmap Masking Algorithm

A digital bitmap masking algorithm was developed to solve problems related to drop placement accuracy, deposited ink amount and drop deposition sequence. The masking algorithm was developed somewhat through trial and error during the layout printing tests of the flex module. Many major and minor tweaks were made

along the way to make the algorithm work with the selected materials and the used circuit layout. The circuit layout files were converted from vector format to bitmap format in 5050 dpi resolution. The the converted images were masked by a bitmap mask. The mask is constructed as follows (see figure 3.12). A pixel formation is placed in a 37 by 37 pixels element and it is tilted in order to place adjacent pixels in different rows. Pixels are placed ca. $31\mu m$ from each other. This corresponds approximately with the drop spacing in 800 dpi resolution. Another similar mask layer is placed within the pixel element to enable sufficient ink amount and to even out the pixel distribution within the mask. Thus one printed layer using this mask is equivalent to two layers printed in 800 dpi resolution in ink quantity.

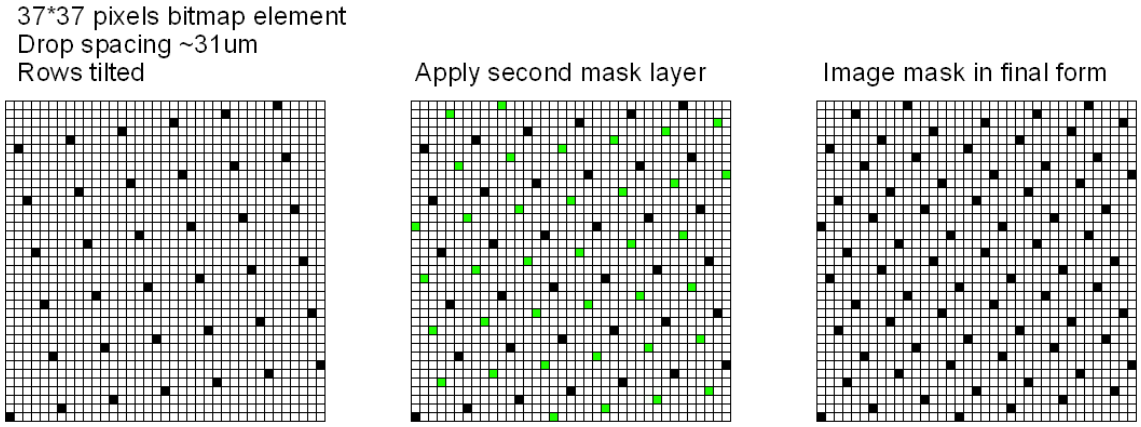

Figure 3.12: Construction of the used image masking pattern.

The masking algorithm masks most of the dark pixels white to lower the amount of ink deposited on the substrate. This way the drop placement accuracy of 5050 dpi resolution can be attained while deposited ink amount is also controlled. The printing sequence using the masking algorithm is presented in figure 3.13.

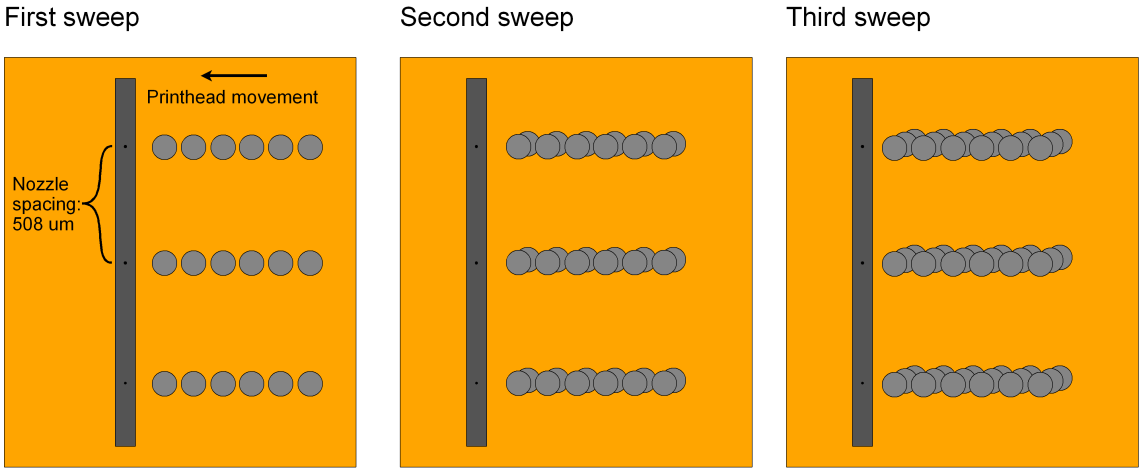

Figure 3.13: Image construction by using the masking algorithm.

The remaining pixels are placed so that the spacing of pixels located on the same

row is greater than the ink drop diameter on the substrate. Due to this, the drops that are printed on the same sweep do not overlap and the drops are allowed to dry individually. If the drops are to be connected, it will happen with the drops printed on the next couple of rows. The drop delay between adjacent drops is now roughly in second scale both in process and cross-process directions. This leads to a stacked coin like structure all around the inkjetted circuit while bulging and flooding phenomena have been eliminated. As a conclusion different design phases are presented in figure 3.14 along with examples of the circuit layout and the inkjetted circuit in its final form.

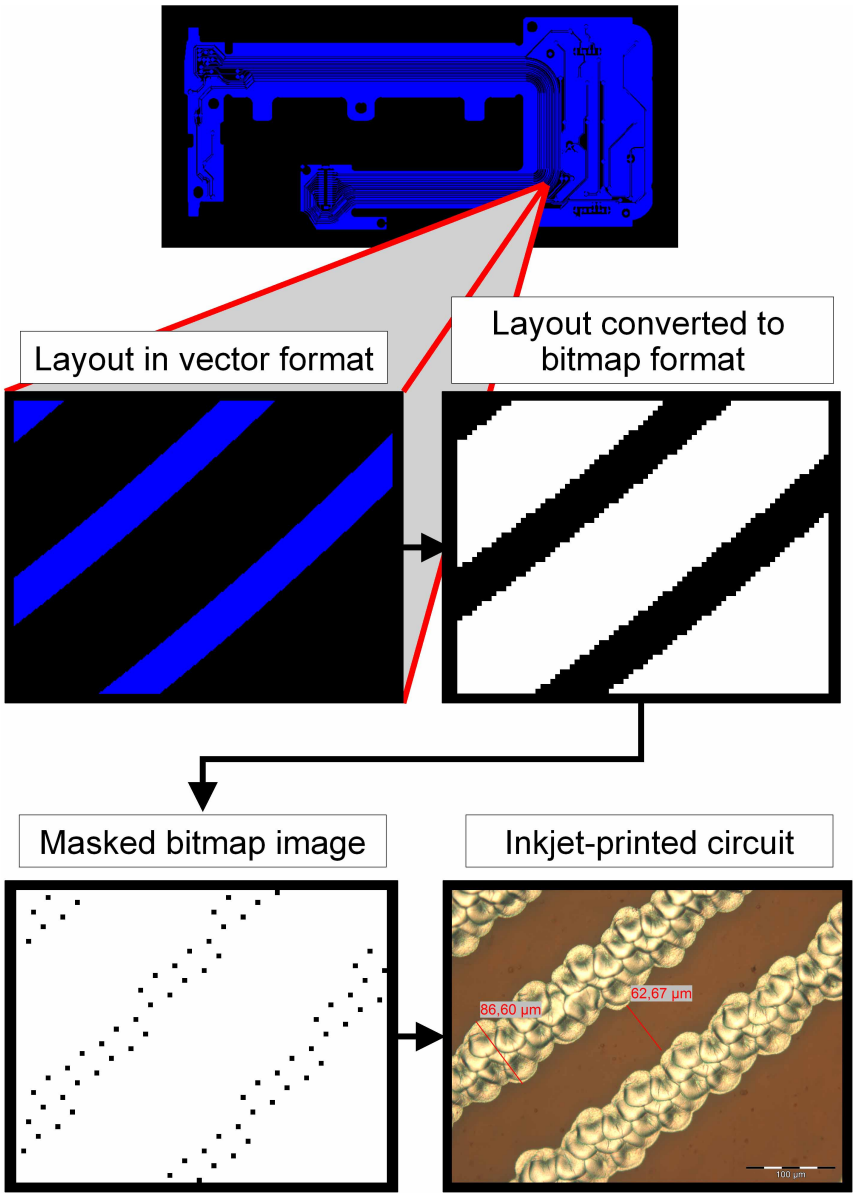

Figure 3.14: Phases of the layout design process and inkjet printed circuit. The used image is a close up of the originally 75 μm wide traces in the layout.

4. PRINTED FLEXMODULE ASSEMBLY

In this chapter the assembly process of the demonstrator device is described and the various assembly methods and devices are introduced. The goal is to go through the assembly process in detail and give the reader a conception of the steps needed to manufacture a product by the means of printable electronics. However, it is important to keep in mind that the assembly process is dependant on the product requirements and some of the steps described in this chapter might not be needed for another product, while some other steps may need to be applied. Overview of the manufacturing process can be seen in figure 4.1.

4.1 Kapton Polyimide Preheating

The first step of the assembly process was preheating of Kapton film. Preheating on Kapton polyimide is needed because of the shrinkage of Kapton in oven during the sintering of NPS-J silver ink. The relative shrinkage of 50 μm thick Kapton has been determined to be 0.22 % in the horizontal direction and 0.11 % in the vertical direction of the Kapton film, when Kapton is heated for 60 minutes in 220 °C. Horizontal direction is the direction in which Kapton is rolled into a roll.

Preheating of Kapton was decided to be used because the assembly process contains separate heating processes. Without preheating the shrinkage would cause errors in the design dimensions between the sintering of top and bottom layers of the flexible PCB. The PCB design file is about 81 mm in length and 40 mm in width. In the worst case scenario with 0.22 % shrinkage would result in about a 170 μm error in the length of the PCB. While it can be argued if preheating was necessary for this specific application, it was decided to be used as a precaution to accumulate as little dimensional error as possible. Kapton was precured for 15 minutes in 220 °C. This was noticed to be sufficient to eliminate the effects caused by shrinkage of Kapton.

Thinking from a manufacturing point of view, eliminating the need for substrate preheating is desirable. As discussed, the need for substrate preheating in this application arose because of the substrate shrinkage during the sintering of the first conductive layer. Substrate shrinking causes dimensional error between the first conductive layer and the second conductive layer. This can be seen as a mismatch of dimensions when aligning the first and second conductive layers. It is significant

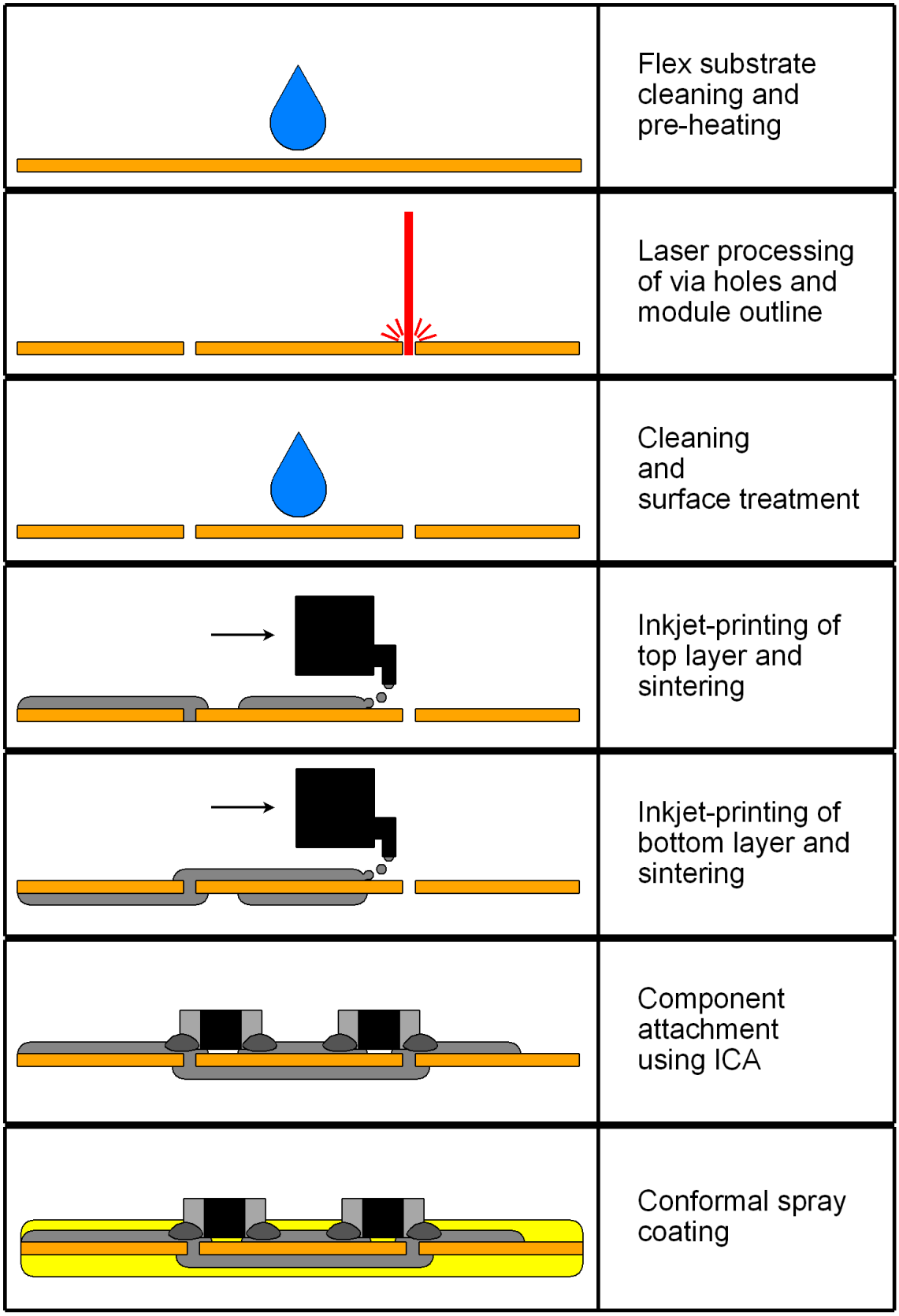

Figure 4.1: Manufacturing phases of the flex module.

in this application because the pad coordinates must match. However, the via pad sizes allow a small dimensional mismatch as the diameter of the pad is about 600μm.

It could be possible to eliminate the need for substrate preheating in the design phase or in the assembly phase. One way of compensating the dimensional error caused by substrate shrinking is to scale the first inkjetted layer larger so that it would shrink back to its intended size with the substrate during the first sintering cycle of the assembly. Other way would be to combine the sintering phases of top and bottom conductive layers into one sintering phase. This would mean that after printing the first conductive layer is dried but not sintered during the printing of the second conductive layer. Unsintered NPS-J withstands some amount of handling on polyimide, but bending the substrate much will result in separating the ink from the substrate. Therefore flipping the substrate over during assembly while having unsintered ink on it might be difficult to carry out.

4.2 Laser Processed Vias and Module Outline

The via cutting and module outline cutting was done in the same phase with a picosecond scale pulse laser. The laser has 2 W output power and it operates in 1064 nm wavelength. The laser uses a mirror scanner module (see figure 4.2) to control the laser beam movement to create patterns on a substrate. Focus depth and planar translation are controlled with a three-axis micrometer table. The via drill file from the original design was used to create the processing file for X-lase laser. Via holes were replaced by circles with a diameter of 150 μm.

The module outline was partially cut out from the substrate, but it was left intact at some points (see figure 4.3). This way the module remained attached to the substrate for the entire production phase. This was helpful when attaching the substrate to iTi inkjet printer vacuum table as experience showed that a entirely cut module would not stay flat on the vacuum table. Align marks for the alignment of inkjetted conductor layers were made at each end of the laser cut design. Due to the small processing area of the scanner module (5.5 cm^2) the processing had to be done in two parts. First the other end of the layout was processed, then the substrate was moved 4 cm and the rest of the layout was processed. Due to small offset between the micrometer table translation axes and scanner module beam movement axes, an offset vector was visually determined to be used in the laser scanner control file to correct the placement error. Due to the scanner head operation and the large processing area, pincushion and barreling effect if the processed pattern was observed. Pincushion and barreling effects cause curvature of straight lines in the edges of the processing area. This also affected the coordinates of the via holes, which needed to be manually corrected, so that they would match the routing conductive layers later printed with the inkjet printer.

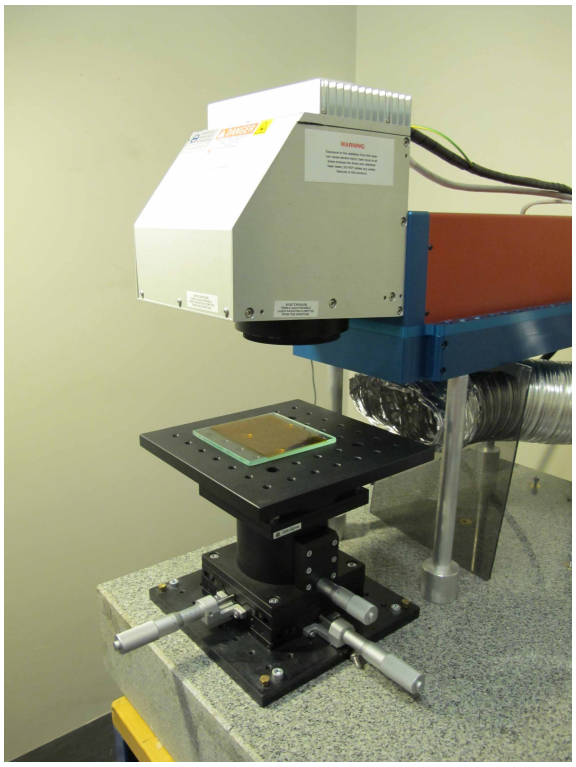

Figure 4.2: Sample processing with Corelase X-Lase.

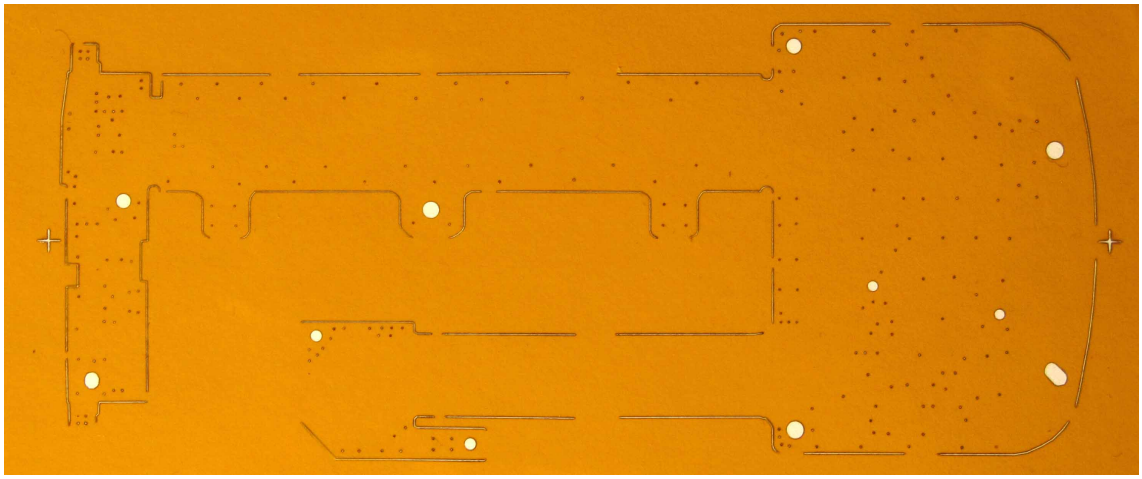

Figure 4.3: Laser cut flex module outline and laser drilled vias.

4.3 Inkjetted Circuit Board

The conductive layers of the PCB were made by iTi inkjet printer (see figure 4.4). The equipment consists of the printer and the controller units for the printhead and XY-table. Separate software and control units are used control the XY-table and the Spectra printhead to produce inkjetted patterns. A Spectra SQ-128 jetting assembly was used in the Spectra printhead.

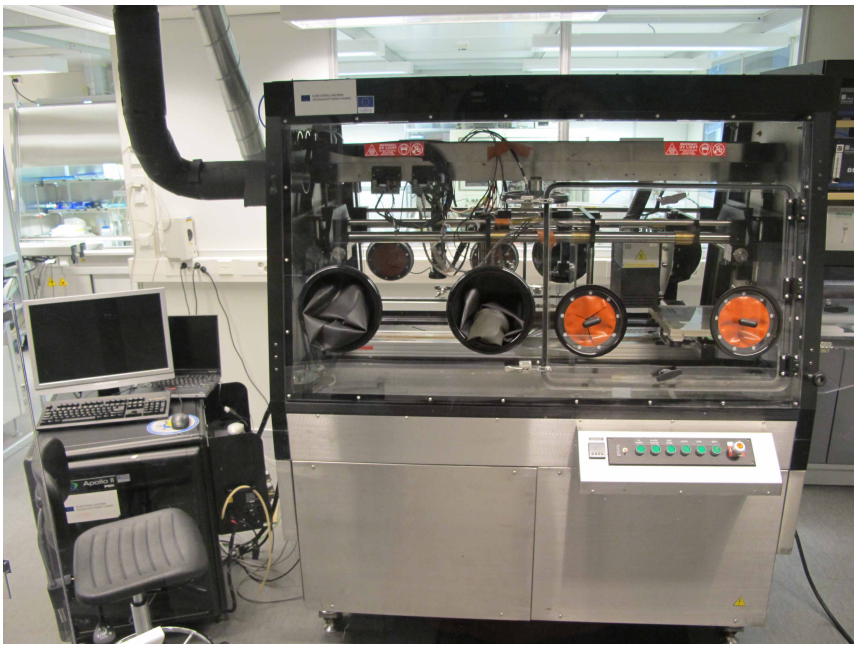

Figure 4.4: iTi inkjet-printer and control module.

The temperature of the printhead can be controlled to obtain optimal ink jetting conditions. Ink jetting can be tuned also by controlling the firing voltage pulse amplitudes and pulse waveform. Ink behavior on substrate is controlled by adjusting the substrate temperature and printing speed. Printing parameters can be optimized by using a drop watcher device. The printing parameters used to print the conductive layers of the flex module are listed in table 4.1. Before printing the substrates were cleaned with isopropanol and a 1% EGC-1720 surface treatment was made. After printing the samples were sintered in 220°C for 60 minutes.

With optimized printing parameters and the image masking algorithm the inkjetting of the layout was possible. In the early trials when the layouts were printed without the masking algorithm the print quality was not good enough for this specific layout with the used equipment. Example of the print quality achieved with the masking algorithm can be seen in figure 4.5

Printing parameters	
Piezo pulse amplitude (V)	45
Pulse rise time (ms)	8
Pulse width (ms)	2
Pulse fall time (ms)	2
Printhead temperature (°C)	45
Print plate temperature (°C)	70
Printing speed (mm/s)	30

Table 4.1: Printing parameters used to print the conductive layers of the flex module.

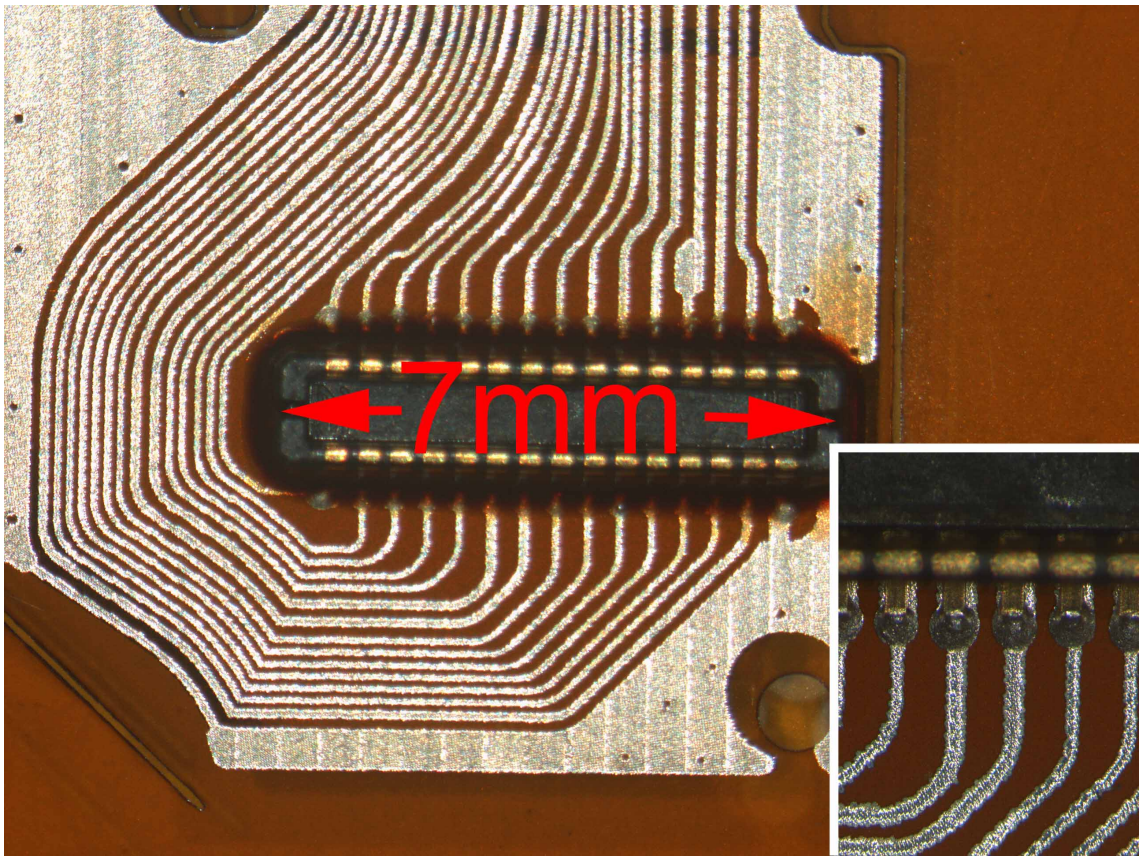

Figure 4.5: Example of fine pitched traces in the layout. The thinnest traces are about 90 μm wide.

4.4 Component Attachment

The component attachment was done with ICA and two component epoxy. ICA was used to make the electrical connections between the components and the circuit and epoxy was used to enhance the durability of the mechanical joint between the component and the substrate. Overview of the deposition process is presented in figure 4.6. ICA and the epoxy material were dispensed by a handheld pneumatic fluid dispenser so that the amount of dispensed material could be controlled by the pneumatic pulse length. Components were placed by hand or by Fineplacer component placement tool. The ICA joints were cured in a convection oven for 15 minutes in 150 °C. After the ICA curing two-component epoxy material was deposited around the components to improve the mechanical joint of the component and the substrate. During the assembly of the first prototypes it was noticed that some components, especially the larger ones, would snap off from the substrate during bending. Epoxy mold around the components helped to keep them attached to the substrate very well. After the epoxy is cured around the components, it acts as a stiffener preventing the substrate from bending under the components. This takes the strain off from the components joints and prevents the components from detaching. Epoxy material was also deposited with a pneumatic dispenser and it was cured in a convection oven for 10 minutes in 150 °C.

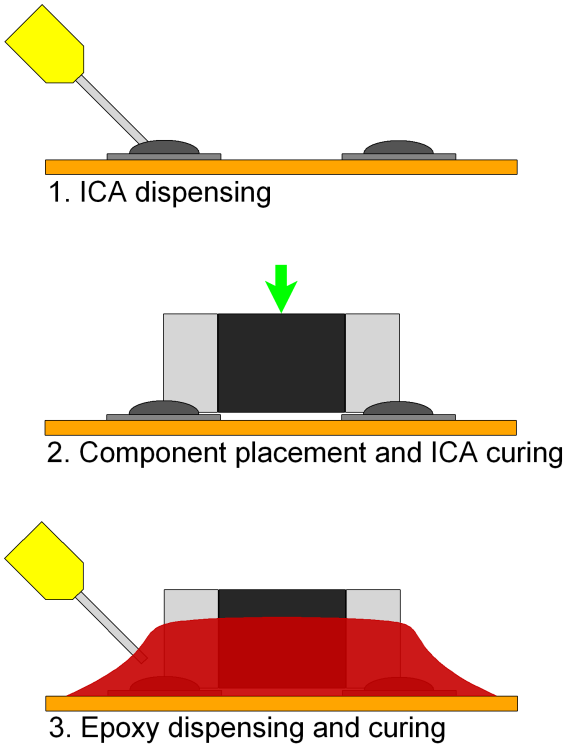

Figure 4.6: Component attachment steps.

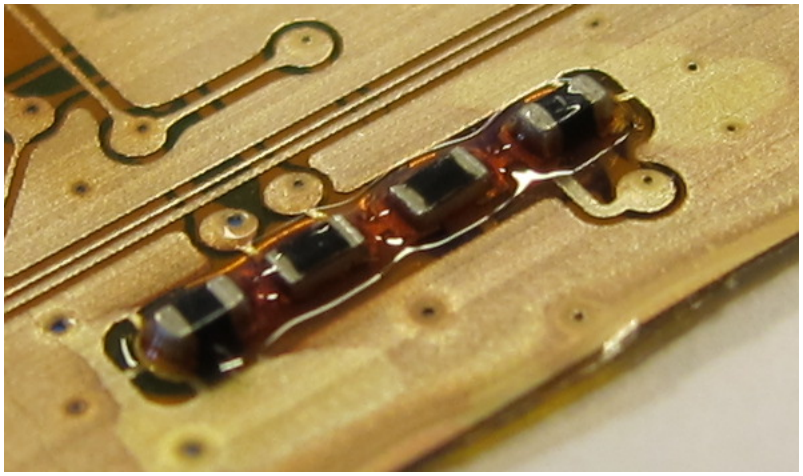

Figure 4.7: Components attached to an inkjetted flex module using ICA and epoxy material.

4.5 Conformal Coating

After the component attachment the flex circuit were covered with a spray-on conformal coating (see figure 4.8). One side was sprayed and allowed to dry and then coating was repeated on other side. This phase of the assembly work was probably the most irreproducible due to the fact that the spraying process is much dependant on the operator. Also pieces of plastic were used to mask out larger areas of the flex circuit, e.g. the connectors which needed to be protected from the spray coating. Even though in the unmasked areas the spray coating resulted in an even layer of coating, around the masked areas there was a lot of variance in the quality of the coating. The other hindsight with this method is that some of the grounding points which connect the flex module ground layer to the metal frame of the phone were left out due to practical reasons. An alternative coating method would be inkjetting the coating layer. By doing this the shape of the coat could be controlled and the masking problems could be avoided. However considering the timetable and due to practical reasons, a spray-on coating was decided to be used, even though it may not be the best alternative. By using a spray-on coating a dielectric layer could be created to protect the traces on the flex module mechanically and also to separate them from the metal frame and other parts of the phone.

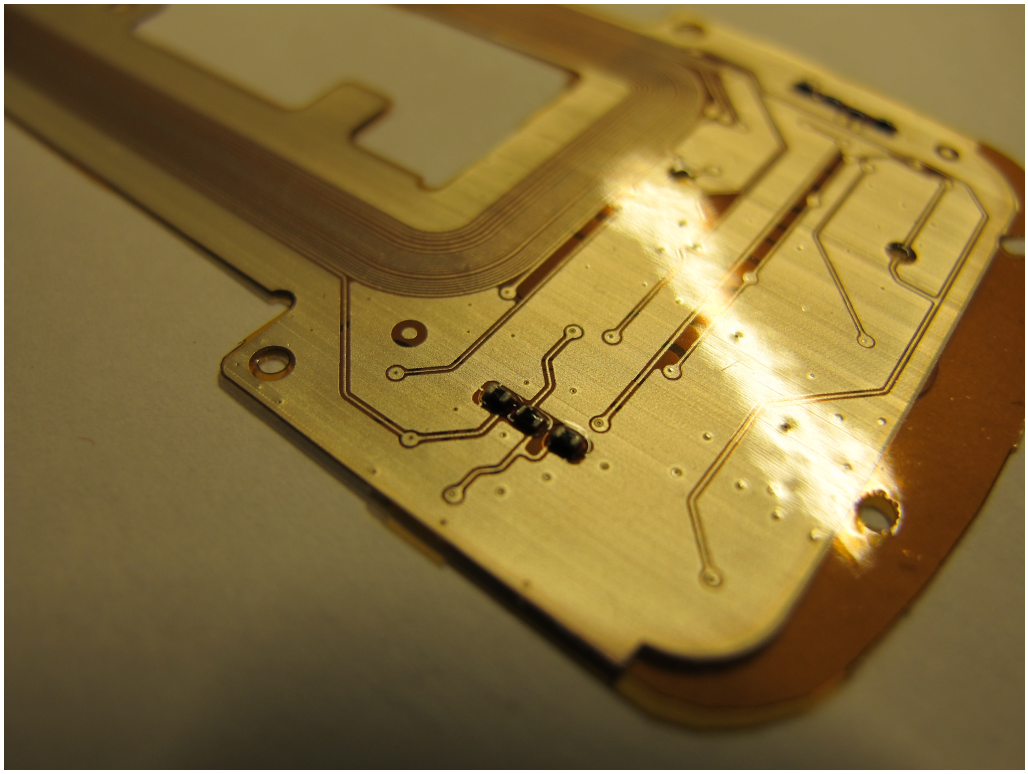

Figure 4.8: Flex module after conformal coating.

4.6 Stiffener Plates Laser Processing

The flexible PCB has two stiffener plates under both connectors. Stiffener plates are used to reduce the mechanical stress inflicted upon the solder joints or in this case ICA joints. The stiffener plates proved out to be important while connecting the flexible PCB to the motherboard and while connecting the LCD to the flexible PCB. The plates help provide even force distribution to the connectors while pressing. The motherboard connector stiffener is made out of a 270 μm thick metal plate, which was provided with the components. The stiffener plate under the LCD connector was laser cut out of 100 μm thick polyimide film (see figure 4.9). Both stiffener plates were attached to the PCB with an adhesive film cut out in the shape of the stiffener plate.

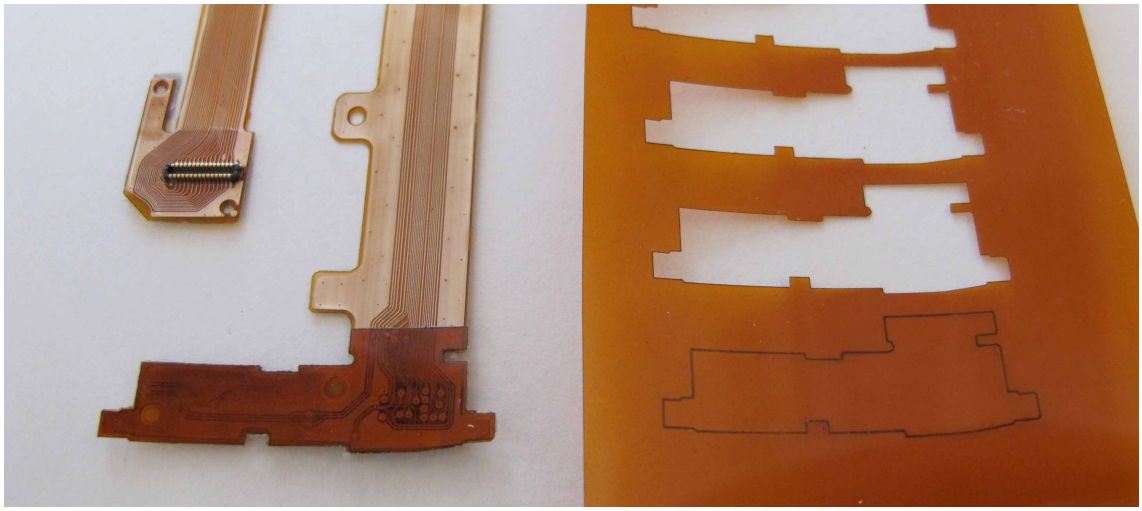

Figure 4.9: A laser cut stiffener plate.

4.7 Mounting the Flexible PCB in the Mobile Phone and Initial Testing

The inkjet-printed flex modules needed to be verified before sending them for further testing to the manufacturer. Initial testing was done by measuring signal lines for short circuits and open circuits. The first inkjetted prototype was tested in a self-built support frame where the flex module could be mounted with minimal stress to component connections and the flexible circuit board. At this point the flex module was connected to the motherboard and LCD but the phone casing was not fitted.

After the electrical functionality of the inkjet-printed flex module prototype was verified a set of new samples were manufactured and mounted inside the actual phones. In order to do this the phones casings were disassembled, the display was disconnected from the flex module and the original flex was disconnected from the motherboard. The circuitry of the flex modules was tested for short circuits and open circuits before installing the flex module inside phone casings. The samples were initially tested by making sure that each phone starts up and that the LCD, keyboard and earpiece were functioning properly. Possibility to make and receive calls was also tested. Eventually 3 working samples were delivered to the manufacturer for further testing.

5. ANALYSIS AND PERFORMANCE TESTING

In this chapter the differences between the original flex module and inkjet-printed flex module are discussed. First the structural differences are compared followed by a series of electrical tests, which aim to point out any differences in performance.

5.1 Structural Comparison

In this section the differences in construction of the inkjetted and original flex module samples are pointed out by cross-sectional images. Layer thicknesses, via structures and component connections are discussed.

5.1.1 Layer thicknesses

Inkjet-printed conductive structures are typically only few a microns thick. Very small amount of conductive material is used compared to e.g. etched circuits. The amount of silver ink used for the both sides of the inkjetted flex module is about 110 microliters. This was calculated by multiplying the amount of pixels in the bitmap files with the average ink drop size. With one liter of silver ink ca. over 9000 pieces could be manufactured if all ink is used for making the flex module. The module thicknesses can be seen in figure 5.1. The total thickness of the inkjetted flex module is about 150 μm. The thickness of the original module is about 120 μm. The inkjetted flex module is slightly thicker because of the thicker substrate material and thicker coating layer.

The difference in conductive layer thicknesses in the inkjet-printed and original flex module can be seen in figure 5.2. In the inkjetted structure the silver ink layer thickness is around 7 μm, which is about one third of the metal layer thickness in the original flex module. In the original flex module the copper layer thickness is about 20 μm.

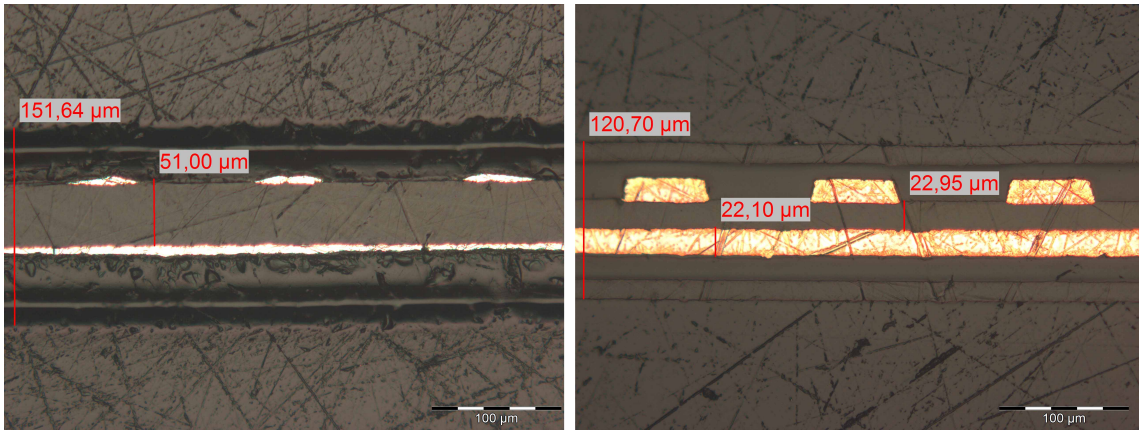

Figure 5.1: Cross-section of the whole flex module. Inkjetted flex module is presented on the left and the original on the right.

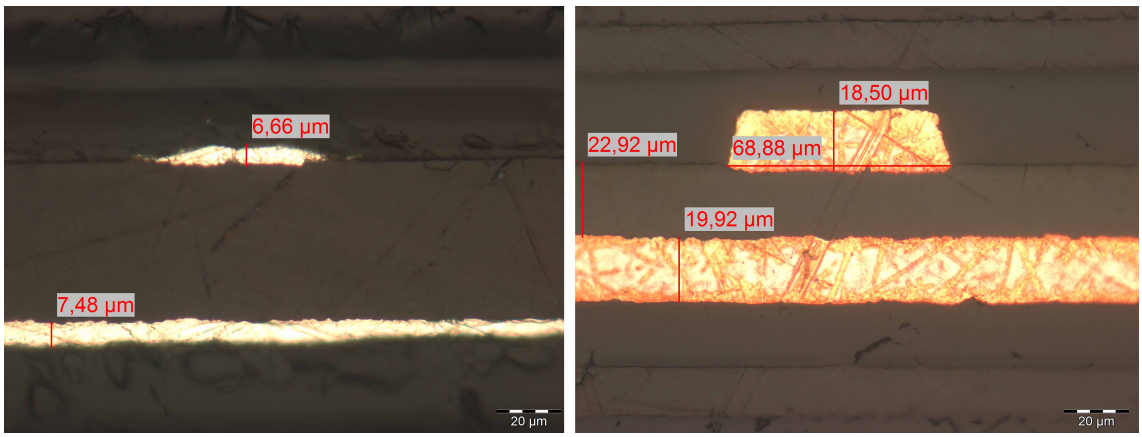

Figure 5.2: Conductive layer thicknesses of the flex modules. The inkjetted flex module is on the left side and the original on the right side. In both pictures the substrate can be seen between the conductive layers. A cross-section of a signal line can be seen on top of the substrate, lower conductor layer is the ground plane.

5.1.2 Via Structures

Cross-sectional images of the via structures in the inkjetted flex module and the original flex module are presented in figure 5.3. Laser drilling of the via holes results in a cone shaped cross-section of the hole. There is no apparent disadvantage of a hole construction like this, on the contrary this helps the ink droplets to land inside the hole also while printing. As the hole is filled with inkjet-printed silver ink, there is no need for filling the holes with conductive any material to make a connection through the substrate. However, this might be necessary from reliability point of view.

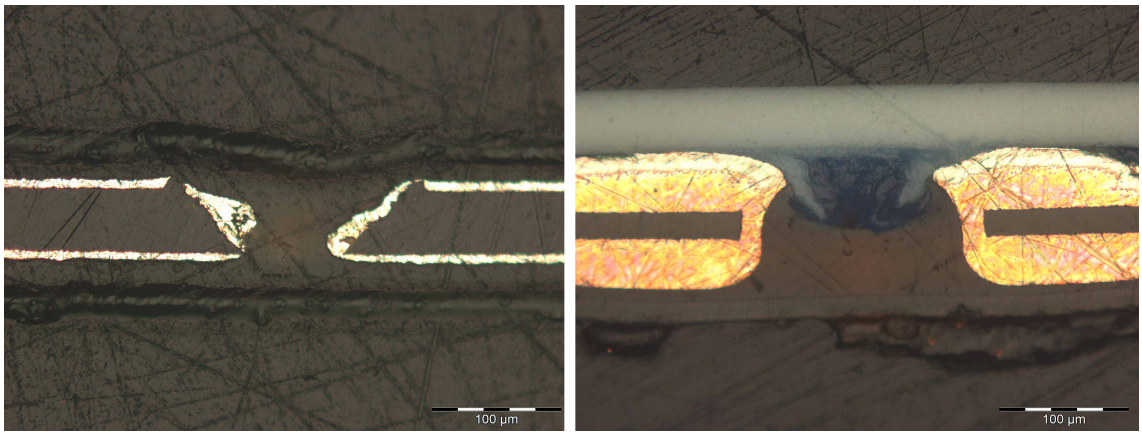

Figure 5.3: Cross-sectional images of the via structures in the flex modules. Via construction of the inkjetted flex module is presented on the left and the original flex module on the right.

A close-up of the edge of the via hole can be seen in figure 5.4. In theory this is the point in the via construction where the conductor layers printed on opposite sides join. In this case the conductor layer is roughly 3-4 μm thick at the point of joining.

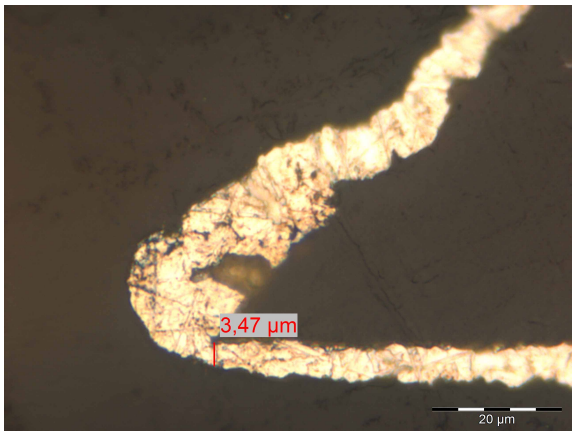

Figure 5.4: Close-up of the sharp edge of the via hole.

5.1.3 Component Connections

Cross-sectional images of the component connections can be seen in figure 5.5. Component connections in the inkjetted flex module were made with ICA and epoxy material. ICA was used to make the electrical connection between the component and the circuit board and underfill material was used to strengthten the mechanical joint of the components and the substrate. The mechanical strength of the ICA glue is not as good as in a solder joint, so strenghtening the mechanical joint with e.g. underfill material is more or less needed depending on the amount of mechanical stress that the component has to endure. In the early prototypes of the inkjetted flex module some components fell off during the mounting of the flex module inside the mobile phone. Dispensing underfill material around the components helped this problem significantly.

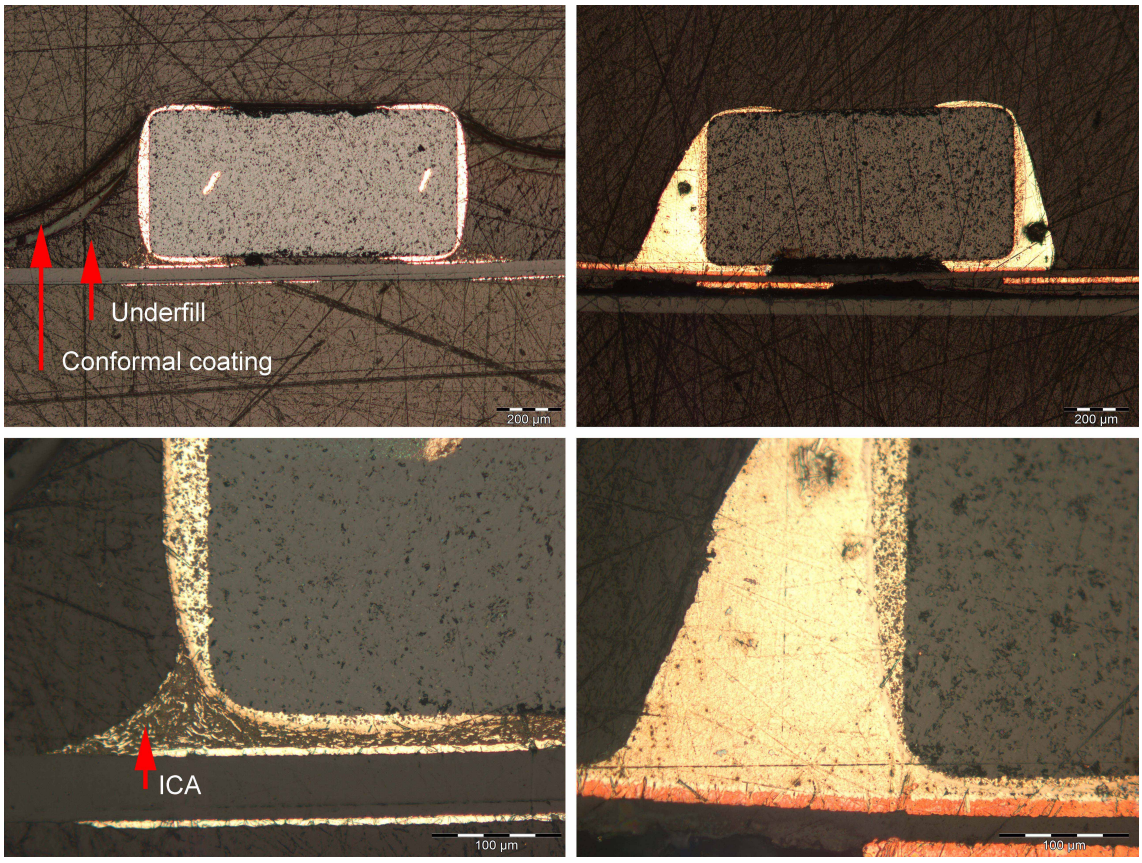

Figure 5.5: Cross-sections of the components connections on the flex modules. Images on the left are taken from the inkjetted flex module and images on the right are from the original flex module. On the left side images the ICA joint and layers of underfill material and conformal coating can be seen. On the right side images the solder joint of the component and circuit can be seen.

5.2 Performance Tests

Three phones fitted with an inkjetted flex module were delivered to the manufacturer of the original flex modules for testing. Tests for electromagnetic compatibility (EMC), electrostatic discharge (ESD), antenna performance, display interface timings and audio quality were made. The phones will be referred as phones A, B and C in this section. A list of phones used in each test is presented in table 5.1. When possible, measurements made with a phone fitted with an original flex module are presented as reference. The terms type approval (TA) and standard product requirements (SPR) will be used in this chapter to express the test results. TA limits are determined by standards, like for example the IEC (International Electrotechnical Comission) standard EN55022 in the case of EMC tests. SPR are internal standards used by the manufacturer and are usually stricter than TA limits in order to prevent any surprises when applying for TA for a certain device.

Test	Samples
EMC	B,C
ESD	B,C
Antenna	A,B,C
Display	B,C
Audio	A,B,C

Table 5.1: List of samples included in the tests

The aim of the tests is to find out if the performance of the flex module has been affected by the changing of manufacturing technology. As can be seen from the cross sectional images, the thickness of the conductive layer is much thinner in the inkjetted flex module than in the original. The resistances of the narrowest signal lines between the two connectors on the inkjet printed flex module are ca. 4 times higher than in the original flex module. Also other structural differences could affect the performance. The components are connected with ICA paste instead of solder and the coating material is different. There is also quite a lot of variance in the assembly of the flex modules as the modules were partly hand made and the effect of the operator is significant.

5.2.1 EMC Test

The purpose of the EMC tests is to find out if there are any harmful emissions caused by the change in the flex module manufacturing technology. The EMC tests were done in two parts. In the radiated spurious emissions test (RSE) phones were tested in transmit mode and receive mode in both GSM-900 and DCS-1800 frequency bands. RSE test emission limits are governed by the ETSI TS 151-010 standard [29]. In radiated emissions (RE) phones fitted with an inkjetted flex module were tested in GSM-900 and DCS-1800 frequency bands. The emission limits in the RE test are governed by the EN-55022 standard [30].

Radiated Spurious Emissions Test

The radiated emissions were measured from two phones fitted with an inkjetted flex circuit in transceiver transmit and receive modes. Measurements were done with phones operating in GSM-900 and DCS-1800 frequency bands. An AC-charger and a headset are connected to the phone during the tests. The measurement setup and the emission limits are described by the ETSI TS 151-010 standard [29]. The RSE test measurement figures and tables can be found in appendix A.

The measurements for phones B and C operating in GSM-900 band in receive mode can be seen in figures A.1 and A.2. The highest measured emission peaks seen from the figures are listed in tables A.1 and A.2. No emissions exceeding the limits were measured.

The measurements for phones B and C operating in GSM-900 band in transmit mode can be seen in figures A.3 and A.4. The highest measured emission peaks seen from the figures are listed in tables A.3 and A.4. The harmonics of the GSM-900 band can be seen in the figures, but the peaks do not exceed the emission limits. The emission spectra of the two phones resemble each other.

The measurements for phones B and C operating in DCS-1800 band in receive mode can be seen in figures A.5 and A.6. The highest measured emission peaks seen from the figures are listed in table A.5. No emissions exceeding the limits were measured.

The measurements for phones B and C operating in DCS-1800 band in transmit mode can be seen in figures A.7 and A.8. The highest measured emission peaks seen from the figures are listed in tables A.6 and A.7. The harmonics of the DCS-1800 band can be seen in the figures, and in the case of phone B the peak of the 2nd harmonic of the operating band exceeds the allowed SPR emission limit by 1.6 dB. However, there is still a 4.4 dB margin to the type approval limits. Sample C passed the SPR limits also in this measurement. The cause for the reduced performance in DCS-1800 band is unclear after the tests. The most probable cause is poor grounding

of the flex module to the device metal frame due to manual assembly of the phones.

Radiated Emissions Test

In the radiated emissions test phones B and C were tested in GSM-900 and DCS-1800 bands. During the tests a call was established. Measurement results for phones B and C operating in GSM-900 band can be seen in figures B.1 and B.2 in appendix B. The highest peaks are listed in tables B.1 and B.2.

Measurement results for phones B and C operating in DCS-1800 band can be seen in figures B.3 and B.4 in appendix B. The highest peaks are listed in tables B.3 and B.4.

All the peaks that are measured above the emission limits are coming from the operation of the transceiver and can be ignored. Both phones passed the SPR limits in the RE test.

5.2.2 ESD Test

The phones fitted with inkjetted flex modules were subjected to electrostatic discharge (ESD) tests to see possible changes in performance. Two phones were tested by firing an ESD gun to several points in the phone body. Some of these locations are presented in figure 5.6. Both air discharge and contact discharge were tested at various pulse amplitudes. A series of ten ESD pulses were given to a location, after which the phone was discharged by using a grounded brush. During the ESD tests the phones were in call mode and the camera was turned on. Phone A was connected to a DC-charger and phone B was connected to an AC-charger. Possible faults during the ESD test include malfunction of the display panels, call drop, phone reset and malfunctioning camera viewfinder.

The results of the ESD test are presented in table 5.2. Only reproducible faults occurred with +8 kV and -8 kV pulse amplitudes in air discharge test on the phone using a DC-charger. In both cases the reproducible fault was a blank display, which then recovered. The discharge locations were location 3 with +8 kV amplitude and locations 1 and 4 with -8 kV amplitude. All of the locations are along the display panel edges. Non-reproducible faults also occurred with 10 kV, 12 kV and -15 kV air discharge pulses. In these cases the fault was also a blank display, which then recovered. No faults were observed in the contact discharge test.

The conclusion after ESD test is that a phone connected to a DC-charger in call mode and with the camera turned on passes the TA but not SPR. A phone connected to an AC-charger in call mode and with the camera turned on passes TA and SPR.

Figure 5.6: ESD test points on the front panel of the phone.

GSM-900 Call Mode/Camera On								
Air Discharge								
Phone	**8kV**	**-8kV**	**10kV**	**-10kV**	**12kV**	**-12kV**	**15kV**	**-15kV**
C (DC-4)	F (3)	F (1,4)	P* (3,11)	P	P* (11)	P	P	P* (5)
B (AC-3E)	P	P	P	P	P	P	P	P
Contact Discharge								
Phone	**2kV**	**-2kV**	**4kV**	**-4kV**	**6kV**	**-6kV**	**8kV**	**-8kV**
C (DC-4)	P	P	P	P	P	P	P	P
B (AC-3E)	P	P	P	P	P	P	P	P

Table 5.2: ESD test results. F = Failed, P = Pass, P* = Pass (fault not reproducible). The discharge location in which the fault occurred is presented in parentheses (see figure 5.6).

5.2.3 Antenna Test

In order to minimize the size of the antenna element the some PCBs of a mobile phone can be used as radiating elements. Even though there is no actual antenna structure on the flex module it is used as part of the antenna in the phone. The receiving and transmission performance of phones fitted with inkjet-printed flex modules and an original flex module were compared.

Total radiated power (TRP) and total isotropic sensitivity (TIS) measurements are used by the industry to determine the performance of wireless devices. TRP and TIS tests provide data on the performance of the physical layer of the device under testing (DUT). In this case the effects of the antenna and the device body are taken into account. Test setups for TRP and TIS measurement resemble each other. Transmitting and receiving performance is tested from multiple directions around the device and a single value is then constructed from the measurements. CTIA test plan describes two ways of performing the spatial scanning of the DUT. In the conical cut method the DUT rotates around its long axis and the measurement antenna is moved around the DUT in a circle. In the great circle cut method the DUT is rotated around two axes and the measurement antenna remains fixed. The test plan also states that measurement antenna should be capable of measuring orthogonal and linear polarizations. [31]

TRP is used to measure the transmitting performance of a device. According to the CTIA test plan test is done by sampling the radiated power from multiple directions and then integrating the sampled values into one scalar value [31]. Altogether 264 measurements per polarization direction are done and the TRP value is integrated from these. This way the radiated power is tested from multiple directions and it gives a good estimation of the devices transmission performance in a real life situation. TIS is used to describe the receiving performance of a device. TIS value is determined by measuring Bit Error Rate (BER) or Frame Erasure Rate (FER). Altogether 60 measurements for each polarization are made. [31]

Measurements were made in EGSM-900 and DCS-1800 frequency bands. Operation in three channels were measured in both cases. In TRP measurements the phone fitted with an original flex module was compared with three phones fitted with an inkjetted flex module. The results can be seen in table 5.3. As can be seen from the table, the TRP values of the phones with an inkjetted flex-module are in the same level as the TRP values of the original reference.

The TIS results are presented in table 5.4. Only one phone was measured, because TIS measurements take a lot more time than TRP measurements. Also the variance in results of the three inkjetted samples in TRP test was small, so one sample in TIS test was deemed to be enough. The results show that the phone fitted with

	EGSM-900			DCS-1800				
	Ch975	Ch38	Ch124	Ch512e	Ch699	Ch885e	Lo avg.	Hi avg.
Orig.	28,63	28,65	28,47	24,88	25,75	26,51	28,59	25,76
A	28,64	28,79	28,70	28,08	25,84	26,47	28,71	25,83
B	28,73	28,85	28,67	25,40	26,16	26,84	28,75	26,17
C	28,98	29,18	28,99	24,89	25,83	26,69	29,05	25,86

Table 5.3: TRP test results (in dBm).

an inkjetted sample does not perform as well as the original reference. In average, the difference in sensitivity is about 8.7 dBm in EGSM-900 band and 4.2 dBm in DCS-1800 band. While the degradation of TIS in the inkjetted samples did not show in the initial test where calls were made and received with the phones the difference in TIS performance compared with the original device is notable. The reason for TIS degradation is suspected to be an EMC issue, because the TRP values of phones with inkjetted flex modules were good. One possible reason for the change in performance is that the inkjetted flex module prototypes are not grounded against the phone metal frame as well as the original flex modules. Due to practical reasons in the manufacturing of inkjetted flex modules, all grounding points in the flex module were not realizable. Other suspected reason is the quality of the ground layer in the inkjetted flex module. The inkjetted ground layer is about $10\mu m$ thick, whereas the etched copper is about twice as thick. Also the resistivity of inkjetted silver is about $3\mu\Omega\cdot$ cm [22] and the resistivity of bulk copper is about $1.68\mu\Omega\cdot$ cm. However, it is unlikely that the differences in layer thicknesses and resistivities alone are enough to explain the difference in TIS values as the TRP values showed no degradation caused by the change of manufacturing technology.

	EGSM-900			DCS-1800				
	Ch975	Ch38	Ch124	Ch512e	Ch699	Ch885e	Lo avg.	Hi avg.
Orig.	-106,76	-106,32	-106,26	-96,32	-97,62	-94,98	-106,44	-96,18
B	-98,99	-96,78	-97,78	-89,55	-93,07	-95,06	-97,76	-91,95

Table 5.4: TIS test results (in dBm).

5.2.4 Display Test

One functionality of the flex module is to connect the display module to the motherboard of the mobile phone. This is done by 13 data lines. Display testing includes measuring the signal rise and fall times of individual data lines and more complicated interface timings. Measurements were done for phones B and C. This test was particularly interesting because due to the change from a traditional flex module to an inkjetted flex module, the resistances in the data lines grew somewhat

significantly. It was expected that this could affect the signal timings needed for controlling the display.

The interface timing test consists of testing the parallel operation and timings of different data lines. The measurements of the interface timing test and the timing conditions are presented in tables C.1 and C.2 in appendix C. Parallel operation of the display lines for writing on the display was tested. Parallel operation of data/command line, write line and 8 data lines is needed for writing on the display. In this case the critical timing conditions come from the display's datasheet. Sufficient minimum setting times need to be allowed for the signals on different lines. According to the test results the timing conditions were met.

Signal rise and fall times were measured from the data lines on the flex module. The measurements are presented in table C.3 in appendix C. Signal rise time is the time interval between transition from 30% to 70% (70% to 30% for fall time) of the logic power supply voltage, which is specified as 1.65 V - 1.95 V. The timing condition for both the rise and fall time for all the data lines is 15 ns. In all the measured lines the rise and fall times were under 15 ns i.e. the timing condition was met.

The change of manufacturing technology did not affect the interface timings and signal rise and fall times in the display control lines as much as expected. Interface timing conditions and the signal rise and fall timing conditions in the display control lines were met.

5.2.5 Audio Test

The flex module carries the audio signal to the earpiece from the mother board. The audio quality was measured from phones A, B and C to see if the change in flex module manufacturing technology had any effect on the audio quality. Results were then compared with measurements made with an original reference phone.

TDMA Noise

TDMA (Time Division Multiple Access) is a channel accessing method used in GSM networks between the user and the base station. The same frequency channel is used by multiple users by giving them individual time slots inside which they can receive and transmit data to the base station. In the mobile phone hardware level this means that the transceiver needs to operate in fixed time intervals during a phone call. The principle of the transceiver's supply current usage is described in figure 5.7.

Usually the transceiver in a mobile phone operates at a 217 Hz frequency during a phone call. Noise in this frequency is audible to the human ear and can be heard

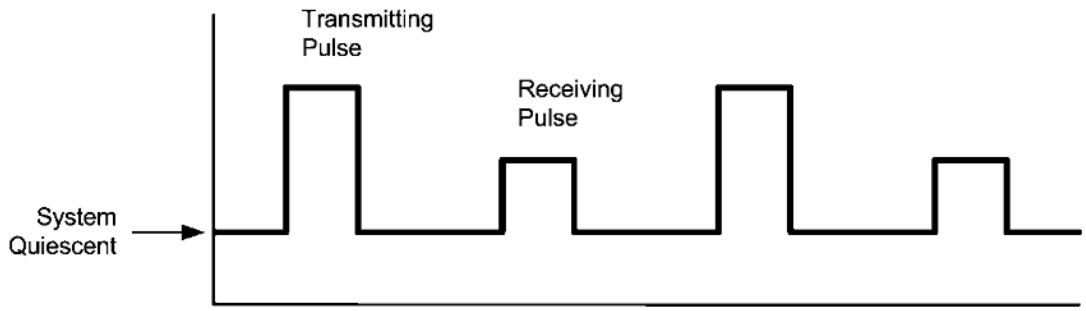

Figure 5.7: Transmitting and Receiving Current Waveform [28]

as a buzzing sound in the phone speaker during a phone call. TDMA noise exists in the mobile phone in two forms: as variations in the DC supply current and as the RF signal's modulation envelope. As the transceiver operates it draws a relatively large current from the DC power supply causing fluctuation in the DC supply current which leads to noise around the circuitry. Additionally part of the transmitted RF energy can couple in the in the audio circuitry. [28]

TDMA noise coupling to the audio circuitry is likely when there are long traces connecting the audio amplifier outputs and the actual speaker element. Long traces act as antennas and if the circuit is designed poorly, noise coupling can have a audible effect on the audio signal quality. TDMA noise can also couple by conduction from the RF components to the audio circuitry and through the ground plane to the audio circuitry. [28]

The TDMA noise level was measured from phones fitted with an inkjetted flex-module and it was compared with a reference phone. Measurements were made from 3 inkjetted prototypes and one original reference case. Both the reference case and one phone with inkjetted flex prototype were measured with the slider open and closed. Measurements were made altogether in six channels. Channel 977 is in the EGSM-900 frequency band, channels 35 and 122 are in the GSM-900 band, channels 514 and 699 are in the GSM-1900 band and channel 883 is in the GSM-1800 band. Measurement criteria for TDMA noise measurements are presented in table 5.5.

Criteria for TDMA measurements			
	Mode	Accepted (dBr, reference 8mV)	Accepted with risk (dBr, reference 8mV)
Uplink	Hand portable	$(-\infty, -40]$	$(-40, -30]$
	Hands free		
	Headset		
Downlink	Hand portable	$(-\infty, -50]$	$(-50, -40]$
	Headset	$(-\infty, -65]$	$(-65, -55]$

Table 5.5: Measurement criteria of TDMA noise measurements for uplink and downlink signal directions in different operating modes.

The test results for down-link and up-link signal directions are presented in tables 5.7 and 5.6. The figures are presented as decibels relative to 8 mV reference level. The noise levels of the measured inkjetted prototypes are acceptable within the measurement criteria in all cases.

Down-Link TDMA noise								
	Band	**Channel**	**Orig. closed**	**Orig. open**	**Inkjet sample C open**	**Inkjet sample B closed**	**Inkjet sample B open**	**Inkjet sample A open**
HP	Low	977	-59	-61	-67	-63	-54	-66
		35	-61	-63	-66	-63	-58	-67
		122	-62	-61	-65	-63	-61	-69
	Hi	514	-61	-69	-73	-70	-70	-71
		699	-60	-70	-72	-69	-70	-73
		883	-60	-68	-71	-67	-68	-71
	Band	**Channel**	**Orig. closed**	**Orig. open**	**Inkjet sample C open**	**Inkjet sample B closed**	**Inkjet sample B open**	**Inkjet sample A open**
HS	Low	977	-72	-76	-67	-72	-76	-76
		35	-70	-67	-66	-70	-67	-70
		122	-76	-79	-75	-76	-79	-78
	Hi	514	-91	-95	-92	-91	-96	-93
		699	-92	-93	-93	-93	-95	-94
		883	-94	-94	-92	-94	-89	-94

Table 5.6: Downlink TDMA noise measurements.

Up-Link TDMA noise								
	Band	**Channel**	**Orig. closed**	**Orig. open**	**Inkjet sample C open**	**Inkjet sample B closed**	**Inkjet sample B open**	**Inkjet sample A open**
HP	Low	977	-50	-47	-51	-50	-51	-51
		35	-51	-49	-52	-51	-52	-53
		122	-51	-50	-53	-51	-54	-52
	Hi	514	-53	-52	-57	-54	-55	-53
		699	-53	-55	-54	-52	-52	-53
		883	-52	-54	-53	-52	-53	-53
	Band	**Channel**	**Orig. closed**	**Orig. open**	**Inkjet sample C open**	**Inkjet sample B closed**	**Inkjet sample B open**	**Inkjet sample A open**
HF	Low	977	-44	**-38**	-43	-43	-42	-41
		35	-49	-41	-47	-44	-45	-43
		122	-48	-43	-47	-43	-47	-46
	Hi	514	-48	-48	-53	-50	-51	-48
		699	-48	-49	-52	-48	-49	-48
		883	-46	-46	-50	-46	-47	-46
	Band	**Channel**	**Orig. closed**	**Orig. open**	**Inkjet sample C open**	**Inkjet sample B closed**	**Inkjet sample B open**	**Inkjet sample A open**
HS	Low	977	-56	-55	-56	-57	-54	-55
		35	-55	-56	-59	-54	-51	-56
		122	-58	-59	-61	-56	-54	-57
	Hi	514	-55	-59	-55	-58	-57	-60
		699	-58	-59	-56	-56	-57	-57
		883	-59	-58	-56	-55	-56	-58

Table 5.7: Uplink TDMA noise measurements. Results are presented as decibels relative to 8 mV reference level. HP = Handheld portable mode, HF = Hands free mode, HS = Headset mode. Low band channels operate in EGSM-900 and GSM-900 frequency bands, High band channels operate in GSM-1900 and DCS-1800 frequency bands.

5.2.6 Summary of Test Results

To conclude the discussion of results, a summary of the test results can be seen in table 5.8. All individual tests are listed and the results are indicated for each of the tested phones. Majority of the tests were passed within the SPR limits. Phone B did not pass SPR limits in the RSE test, but still passed the test within TA limits. Phone C did not pass the ESD air discharge test within the SPR limits, but was within the TA limits. The only case where the performance was reported to be too bad to be accepted was the antenna's TIS test.

The reasons for degraded performance in these cases are not verified. The issue with degraded TIS performance could be related to the fact that the flex modules are likely to be poorly grounded to the metal frame of the phone. Other signals or noise could enter the transceiver through the flex module due to poor grounding. This would lower the sensitivity of the transceiver. One fact that would support this speculation is that the TRP values did not change in the phones fitted with inkjetted flex modules. Within the test results there are no clear indicators that the change in manufacturing technology would affect the flex module performance notably. The observed performance issues seem to be related to the assembly phase and not the performance of the materials.

Test	**Sample A**	**Sample B**	**Sample C**
EMC - Radiated Spurious emissions		TA	SPR
EMC - Radiated Emissions		SPR	SPR
ESD - Air discharge (DC-charger)			TA
ESD - Air discharge (AC-charger)		SPR	
ESD - Contact discharge (DC-charger)			SPR
ESD - Contact discharge (AC-charger)		SPR	
Antenna - Total radiated power	SPR	SPR	SPR
Antenna - Total isotropic sensitivity		FAIL	
Display (interface timings)		SPR	SPR
Display (rise/fall times)		SPR	SPR
Audio (TDMA Up-link)	SPR	SPR	SPR
Audio (TDMA Down-link)	SPR	SPR	SPR

Table 5.8: Summary of test results. Results indicate if the sample has passed SPR or TA limits.

6. FURTHER DEVELOPMENT

Cost related issues drive the electronics manufacturers to seek cheaper materials for electronics production. Therefore it is important to look for new materials, which could be more cost effective in production. The inkjetted flex module was demonstrated on polyimide film by using nanoparticle silver ink for the conductive layers. As the potential of the manufacturing technology has been demonstrated the next goal is to seek for more cost effective combination of substrate and ink material for a similar demonstrator.

Recent commercially available inks [22] enable processing on low temperature substrates, such as PET or PEN, which tend to be cheaper than polyimide. Also in the near future it might be possible to manufacture the conductive layers by using copper nanoparticle ink. Transition from silver ink to copper ink is interesting e.g. because of the difference in bulk prices of the metals. Currently the bulk price of the metal does not significantly show in the ink prices, as the manufactured ink lots are quite small, but the bulk price may become more significant as the volume of ink manufacturing grows. There are also other drivers for the evaluation of copper inks. Soldering of components on silver ink traces is problematic because of the silver leaching phoenomena [32]. Currently isotropically conductive adhesive needs to be used to connect components to an inkjet printed silver ink circuit. Soldering of components on an inkjetted copper ink circuit might be viable. The sintering of dispersant-clad nanoparticle copper inks requires a photonic sintering process instead of conventional heat sintering. Sintering needs to be done rapidly in order to prevent the copper nanoparticles from oxidising during sintering.

One thing related to this work that was left unclear and would need further attention was the mechanical endurance of the inkjet printed key pads. Due to the thinner metal layer it is possible that the pads would wear out during long time use. This was not observed during the testing phase, but long term behavior is unknown.

7. CONCLUSIONS

The target of this thesis work was to manufacture a functional flex module demonstrator by the means of inkjet-printing and other novel technologies and analyze the performance of the flex module with a series of electrical tests. This target was reached.

In the course of this thesis work, a conventional design was transferred to novel manufacturing methods. A set of demonstrator devices were then manufactured and tested. During the design transfer process and manufacturing process knowledge related to designing circuits for printable electronics was gained. Also many novel manufacturing methods were demonstrated. Laser cut via holes filled with inkjetted ink were used to connect grounding layers and signal routings. An inkjet printer was used to manufacture the conductive layers of the PCB and an image masking method was introduced for improving printed image quality. ICA and epoxy underfill were used to create conductive and mechanical joints between the PCB and the components. The assembly process was mainly successful in the sense that the original construction of the flex module was reached. A compromise was made in the making of the conformal coating layer, where some grounding points were left out of the flex module samples.

The testing phase gave much valuable information on the performance of an inkjetted flex module compared with the original flex module. The outcome of the testing phase was good and positive in general. Majority of the tests were passed within the SPR limits and on two test cases within TA limits. On antenna TIS test there was a notable drop in performance and the reason for this is unverified. After discussion with the testing personnel the cause is suspected to be related to EMC issues rather than the performance of the conductive layer as the TRP performance was not affected. In the light of these test results it can be said that inkjet-printing is one viable method for manufacturing flexible circuits such as this demonstrator case. There is still much room for optimization and development in the processes and methods described in this work, but one should keep in mind that the manufacturing was done on research equipment and the input of the operator was quite significant.

In the near future more cost effective materials will be evaluated through a similar demonstrator case. Valuable feedback was gained from the testing phase for issues to be taken into account in the design and manufacturing phase of the future

prototypes. Probably most room for improvement is in the manufacturing of the solder mask. The spray-on conformal coating is problematic because of the masking needed to protect certain areas of the layout. Also due to this coating method some of the grounding points needed to be left out from the inkjet-printed prototypes which showed in the testing results.

REFERENCES

[1] Ville Pekkanen, Matti Mäntysalo, Kimmo Kaija, Pauliina Mansikkamäki, Esa Kunnari, Katja Laine, Juha Niittynen, Santtu Koskinen, Eerik Halonen, Umur Caglar, Utilizing inkjet printing to fabricate electrical interconnections in a system-in-package, Microelectronic Engineering, Volume 87, Issue 11, November 2010, Pages 2382-2390, ISSN 0167-9317, 10.1016/j.mee.2010.04.013. Available at http://www.sciencedirect.com/science/article/pii/S0167931710001383. Referred 4.10.2011.

[2] Manfred Mengel, Ivan Nikitin, Inkjet printed dielectrics for electronic packaging of chip embedding modules, Microelectronic Engineering, Volume 87, Issue 4, April 2010, Pages 593-596, ISSN 0167-9317, 10.1016/j.mee.2009.08.033. Available at http://www.sciencedirect.com/science/article/pii/S0167931709005607. Referred 4.10.2011.

[3] Kimmo Kaija, Ville Pekkanen, Matti Mäntysalo, Santtu Koskinen, Juha Niittynen, Eerik Halonen, Pauliina Mansikkamäki, Inkjetting dielectric layer for electronic applications, Microelectronic Engineering, Volume 87, Issue 10, October 2010, Pages 1984-1991, ISSN 0167-9317, 10.1016/j.mee.2009.12.028. Available at http://www.sciencedirect.com/science/article/pii/S0167931709008715. Referred 4.10.2011.

[4] Kang-Jun Baeg, Dongyoon Khim, Ju-Hwan Kim, Minji Kang, In-Kyu You, Dong-Yu Kim, Yong-Young Noh, Improved performance uniformity of inkjet printed n-channel organic field-effect transistors and complementary inverters, Organic Electronics, Volume 12, Issue 4, April 2011, Pages 634-640, ISSN 1566-1199, 10.1016/j.orgel.2011.01.016. Available at http://www.sciencedirect.com/science/article/pii/S1566119911000310. Referred 4.10.2011.

[5] Pekkanen, V. Mäntysalo, M. Mansikkamäki, P. Design Considerations for Inkjet Printed Electronic Interconnections and Packaging. IMAPS 40th International Symposium on Microelectronics. Nov. 11-15, 2007, San Jose, California, USA. 8 p.

[6] Editors: William S. Wong, Alberto Salleo. Flexible Electronics: Materials and Applications. Springer, 2009. 462 p.

[7] Fjelstad, J., September 2006. Flexible Circuit Technology , 3rd edition. Oregon US, BR Publishing, Inc. 226 pages.

[8] Steve Jurvetson. 23 November 2004. Picture of a flexible PCB on Olympus Stylus camera. Menlo Park USA. Available at http://www.flickr.com/photos/44124348109@N01/2265519. Referred 25.5.2011.

[9] Pekkanen, V., Characteristics of Inkjet Material Deposition for Microelectronics Packaging, Thesis for the degree of Doctor of Science, Tampere 2011, Tampere University of Technology. 53p.

[10] Plateau, J., Experimental and Theoretical Statics of Liquid Subject to Molecular Forces Only. 1873. Available at http://www.susqu.edu/brakke/PlateauBook/PlateauBook.html. Referred 17.10.2011.

[11] Buffat, P., Borel, J., Size Effect on the Melting Temperature of Gold Particles. Physics Review A, 13(1976)6, pp. 2287-2298.

[12] Ville Pekkanen, Kimmo Kaija, Matti Mäntysalo, Esa Kunnari, Juha Niittynen, Pauliina Mansikkamäki. Functional Fluid Jetting Performance Optimization. Elsevier, Microelectronics Reliability 50, 2010, pp.864-871. Available at http://www.sciencedirect.com/science/article/pii/S0026271410000636. Referred 25.5.2011.

[13] Jean Berthier, Pascal Silberzan. Microfluidics for Biotechnology, 2nd edition. Artech House, 2010.

[14] Fromm J.E., Numerical Calculation of the Fluid Dynamics of Drop-on-Demand Jets, IBM J Res Develop., Vol. 28, May 1984

[15] Jang D., Kim D., Moon J., Influence of fluid Physical Properties on Ink-jet Printability, Langmuir 2009,25,2629-2635.

[16] Hsiao, W.-K., Martin, G.D., Hoath, S.D., Hutchings, I.M., Ink drop deposition and spreading in ink-jet based printed circuit board fabrication, Proceedings of Digital Fabrication 2008, Pittsburgh, Pennsylvania, USA, Sept. 6-11, 2008.

[17] Yangsoo Son, Chongyoup Kim, Doo Ho Yang, Dong June Ahn. Spreading of inkjet droplet of non-Newtonian fluid on solid surface with controlled contact angle at low Weber and Reynolds numbers. Journal of Non-Newtonian Fluid Mechanics Volume 162, Issues 1-3, October 2009, pp. 78-87.

[18] Mancosu, R.D., Quintero, J.A.Q., Azevedo, R.E.S. Sintering, in different temperatures, of traces of silver printed in flexible surfaces. Thermal, Mechanical

and Multi-Physics Simulation, and Experiments in Microelectronics and Microsystems (EuroSimE), 2010 11th International Conference. April 2010. pp. 1-5.

[19] Antonio Scandurra, Giuseppe Francesco Indelli, Noemi Graziana Spartà, Francesco Galliano, Sebastiano Ravesi, Salvatore Pignataro. Low-temperature sintered conductive silver patterns obtained by inkjet printing for plastic electronics. Surface and Interface Analysis volume 42, issue 6-7. February 2010.

[20] Kumpulainen, T., Pekkanen, J., Valkama, J., Laakso, J., Tuokko, R., Mäntysalo, M. Low temperature nanoparticle sintering with continuous wave and pulse lasers. Optics and Laser Technology, 43(3), 2011, 570-576.

[21] Tanja Viiru, Optimization of Nanoparticle Ink Sitering Profile, Bachelor of Science Thesis, December 2009, Tampere University of Technology.

[22] Harima NPS-J nanoparticle ink datasheet. Available at http://www.harima.co.jp/en/products/pdf/16-17e.pdf. Referred 19.5.2011.

[23] Kapton HN datasheet. Available at http://www2.dupont.com/Kapton/en_US/assets/downloads/pdf/HN_datasheet.pdf. Referred 18.5.2011.

[24] Niittynen, J., Pekkanen, V., Mäntysalo, M. Characterization of ICA attachment of SMD on inkjet-printed substrates. (2010) Proceedings - Electronic Components and Technology Conference, art. no. 5490822, pp. 990-997.

[25] Creative 124-08C ICA datasheet. Available at http://www.harima.co.jp/en/products/pdf/16-17e.pdf. Referred 19.5.2011.

[26] Epotek U300 epoxy underfill material datasheet. Available at www.microcure.com/pdf/Epo-Tek%20U300New.pdf. Referred 19.5.2011.

[27] Soltman, D., Subramanian, V., Inkjet-Printed Line Morphologies and Temperature Control of the Coffee Ring Effect. Langmuir, 2008, 24 (5), pp. 2224-2231

[28] Soriano, A., April 28, 2008. National Semiconductor Application Note 1496, Noise, TDMA Noise, and Suppression Techniques. Available at www.national.com/an/AN/AN-1496.pdf. Referred. 23.6.2011.

[29] ETSI TS 151 010-1, version 4.3.0., Digital cellular telecommunications system (Phase 2+); Mobile Station (MS) conformance specification; Part 1: Conformance specification (3GPP TS 51.010-1 version 4.3.0 Release 4) , 2001, available at www.etsi.org

[30] CISPR 22 / SFS-EN-55022, Information technology equipment - Radio disturbance characteristics - Limits and methods of measurement, 3rd edition, 1997-11.

[31] CTIA Test Plan, Test Plan for Mobile Station Over the Air Performance: Method of Measurement for Radiated RF Power and Receiver Performance, 2001, available at http://www.ctia.org/content/index.cfm/AID/10021. Referred 24.8.2011

[32] Hankey, D. L., et al, Thick Film Materials and Processes, in Hybrid Microelectronics Handbook, edited by Sergent, J.E. and Harper, C.A. USA 1995, McGraw-Hill. 768p.

A. APPENDIX

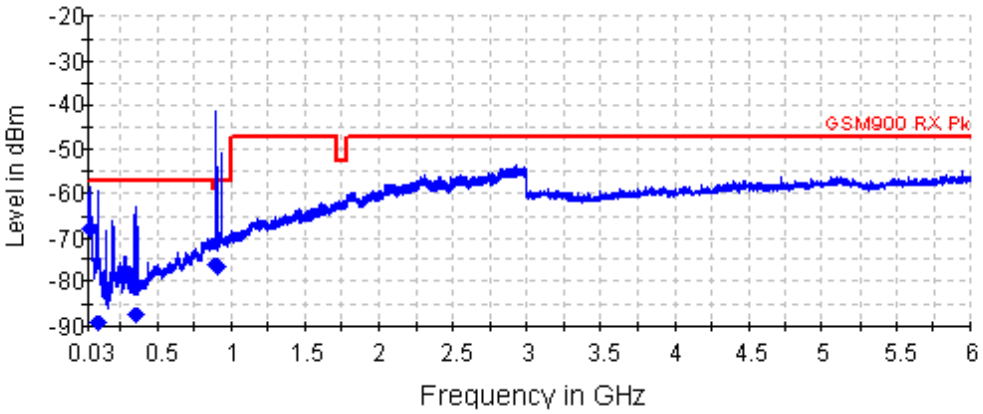

Figure A.1: Phone B, operating in GSM-900 in receive mode. The red line marks the emission limits placed by the ETSI 151 010 standard. The blue line represents the measured emissions.

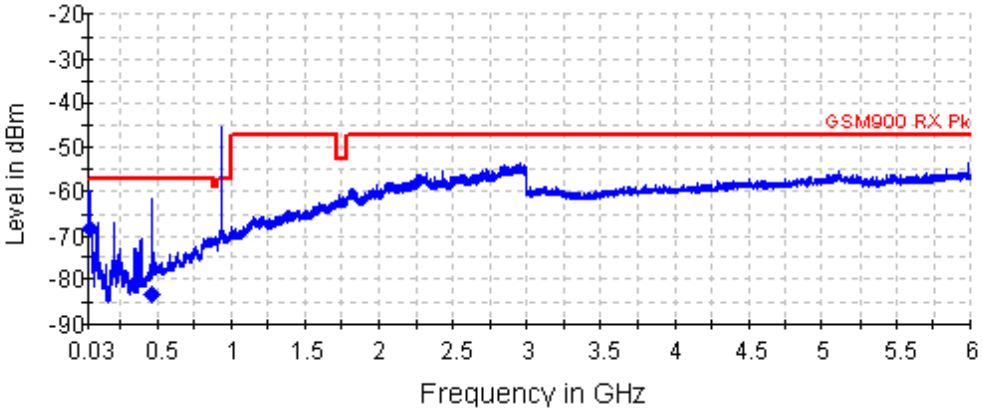

Figure A.2: Phone C, operating in GSM-900 in receive mode. The red line marks the emission limits placed by the ETSI 151 010 standard. The blue line represents the measured emissions.

Frequency [MHz]	**Level [dBm]**	**Margin [dB]**	**Azimuth [deg]**	**Elevation [deg]**	**Polar-isa-tion**	**SPR Result**
40,737	-92,71	29,7	108	0,5	V	PASSED
53,88	-67,92	4,9	102	0,5	V	PASSED
108,18	-89,27	26,3	85	90	V	PASSED
353,303	-87,62	24,6	356	0,5	H	PASSED
892,87	-76,33	11,3	292	90	V	PASSED
899,615	-76,78	11,8	274	90	V	PASSED

Table A.1: Phone B, operating in GSM-900 in receive mode. The Peaks are listed in order by the frequency. 'Level' is the actual peak power and 'Margin' is the margin between the peak level and the allowed emission level. 'Azimuth', 'Elevation' and 'Polarisation' are used to present the direction and polarisation of the emission in respect to the device orientation. A positive SPR result is given if the peak level does not exceed the allowed emission levels.

Frequency [MHz]	**Level [dBm]**	**Margin [dB]**	**Azimuth [deg]**	**Elevation [deg]**	**Polar-isa-tion**	**SPR Result**
30,271	-91,15	28,1	320	0,5	V	PASSED
45,535	-90,71	27,7	90	0,5	V	PASSED
53,693	-68,48	5,5	98	0,5	V	PASSED
464,519	-83,03	20	88	0,5	V	PASSED

Table A.2: Phone C, operating in GSM-900 band in receive mode.

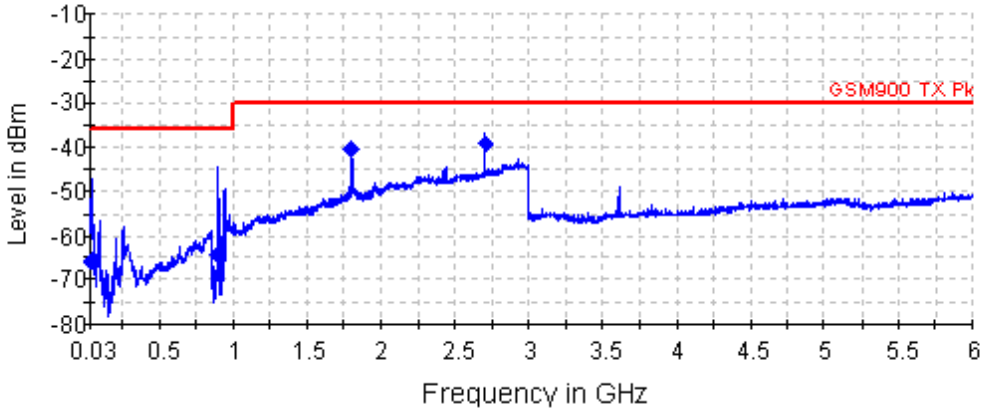

Figure A.3: Phone B, operating in GSM-900 in transmit mode.

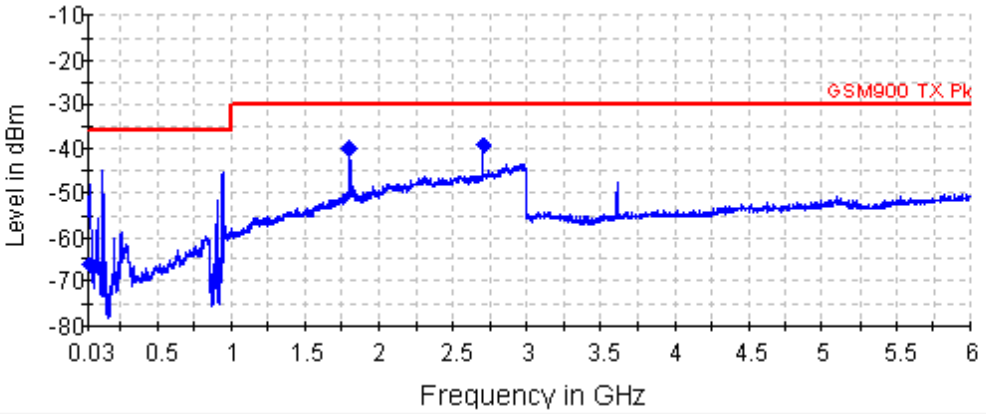

Figure A.4: Phone C, operating in GSM-900 in transmit mode.

Frequency [MHz]	**Level [dBm]**	**Margin [dB]**	**Azimuth [deg]**	**Elevation [deg]**	**Polar-isa-tion**	**SPR Result**
51,774	-65,75	23,80	92	0,5	V	PASSED
51,822	-65,73	23,70	112	0,5	V	PASSED
894,978	-64,42	22,40	130	90	H	PASSED
1804,784	-40,17	4,20	128	90	H	PASSED
2707,457	-39,09	3,10	97	0,5	V	PASSED

Table A.3: Phone B, operating in GSM-900 in transmit mode

Frequency [MHz]	**Level [dBm]**	**Margin [dB]**	**Azimuth [deg]**	**Elevation [deg]**	**Polar-isa-tion**	**SPR Result**
51,289	-66,21	24,2	67	0,5	V	PASSED
134,194	-89,45	47,5	1	90	V	PASSED
1805,004	-40,02	4	222	90	V	PASSED
2706,76	-39,38	3,4	2	90	V	PASSED

Table A.4: Phone C, operating in GSM-900 in transmit mode

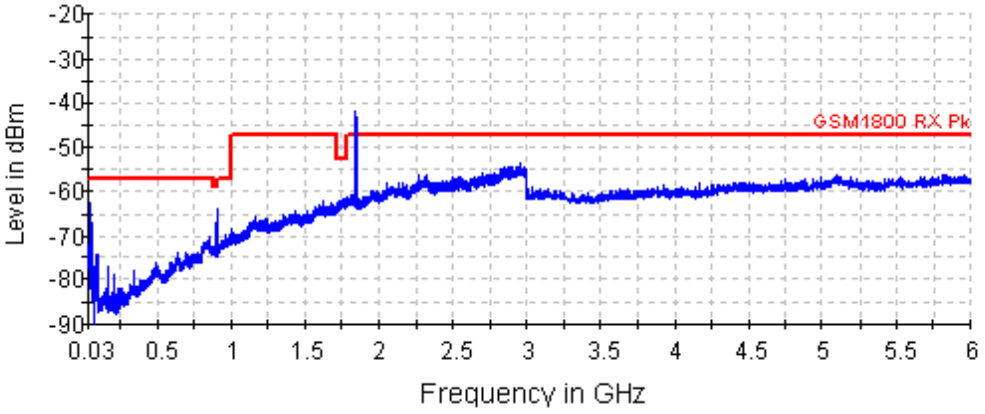

Figure A.5: Phone B, operating in DCS-1800 in receive mode

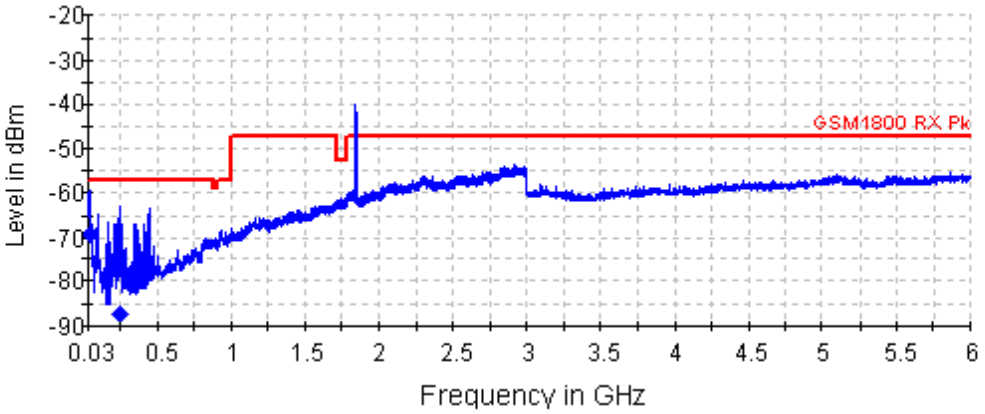

Figure A.6: Phone C, operating in DCS-1800 in receive mode

Frequency [MHz]	**Level [dBm]**	**Margin [dB]**	**Azimuth [deg]**	**Elevation [deg]**	**Polar-isa-tion**	**SPR Result**
33,361	-93,46	30,5	318	0,5	V	PASSED
54	-69,34	6,3	105	0,5	V	PASSED
243,036	-87,01	24	318	0,5	V	PASSED

Table A.5: Phone C, operating in DCS-1800 Receive mode

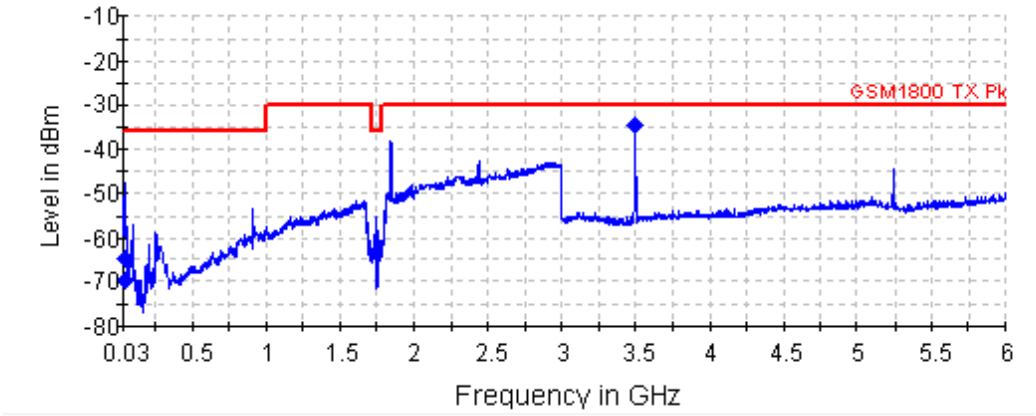

Figure A.7: Phone B, operating in DCS-1800 in transmit mode

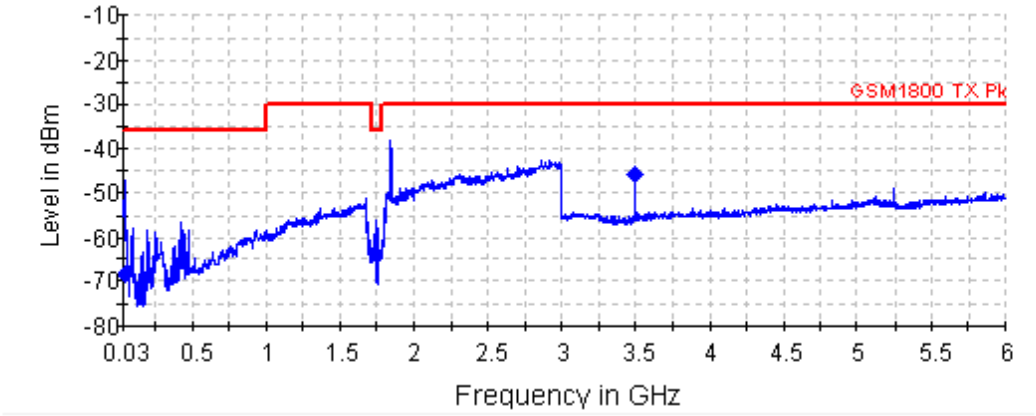

Figure A.8: Phone C, operating in DCS-1800 in transmit mode

Frequency [MHz]	**Level [dBm]**	**Margin [dB]**	**Azimuth [deg]**	**Elevation [deg]**	**Polar-isa-tion**	**SPR Result**
51,517	-69,69	27,7	81	90	V	PASSED
52,335	-64,97	23	112	0,5	V	PASSED
3495,729	-34,37	-1,6	346	90	V	FAIL

Table A.6: Phone B, operating in DCS-1800 in transmit mode

Frequency [MHz]	**Level [dBm]**	**Margin [dB]**	**Azimuth [deg]**	**Elevation [deg]**	**Polar-isa-tion**	**SPR Result**
52,315	-68,47	26,5	92	0,5	V	PASSED
3495,329	-45,8	9,8	173	90	H	PASSED

Table A.7: Phone C, operating in DCS-1800 in transmit mode

B. APPENDIX

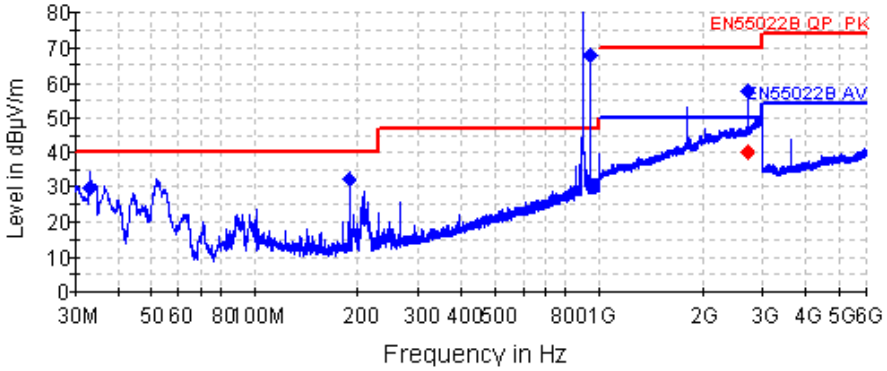

Figure B.1: Phone B Radiated Spurious Emissions (GSM-900 band On). The blue line is the measured spurioud emission spectrum of the phone. Red line marks the EN55022 emission limits.

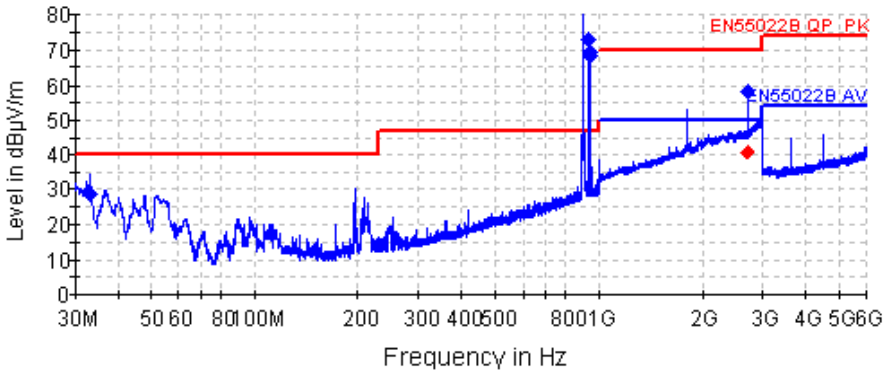

Figure B.2: Phone C Radiated Spurious Emissions (GSM-900 On)

Average						
Frequency [MHz]	**Average [dBμV/m]**	**Margin [dB]**	**Azimuth [deg]**	**Height [cm]**	**Polar-isa-tion**	**SPR Result**
2707,416	40,07	3,9	93	170	H	PASSED
Quasi-peak						
Frequency [MHz]	**Average [dBμV/m]**	**Margin [dB]**	**Azimuth [deg]**	**Height [cm]**	**Polar-isa-tion**	**SPR Result**
33,456	29,49	4,5	269	170	V	PASSED
187,636	32,16	1,8	27	170	V	PASSED
902,535	110,86	-69,9	227	170	H	FAIL (*)
947,455	67,85	-26,9	313	170	V	FAIL (*)
Peak						
Frequency [MHz]	**Average [dBμV/m]**	**Margin [dB]**	**Azimuth [deg]**	**Height [cm]**	**Polar-isa-tion**	**SPR Result**
2707,416	57,58	6,4	93	170	H	PASSED

Table B.1: Phone B Radiated Spurious Emissions (GSM-900 On). Failed peaks caused by the transceiver are marked with '(*)'. The peaks are listed in order by frequency. 'Average' tells the average intensity of the peak. 'Margin' tells the margin to the emission limits set by the standard. 'Azimuth', 'Height' and 'Polarization' tell the orientation and polarization of the emission. 'SPR Result' indicates if the peak has exceeded the SPR limits.

Average						
Frequency [MHz]	**Average [dBμV/m]**	**Margin [dB]**	**Azimuth [deg]**	**Height [cm]**	**Polar-isa-tion**	**SPR Result**
2707,114	40,96	3	45	170	V	PASSED
Quasi-peak						
Frequency [MHz]	**Average [dBμV/m]**	**Margin [dB]**	**Azimuth [deg]**	**Height [cm]**	**Polar-isa-tion**	**SPR Result**
33,377	28,99	5	202	170	V	PASSED
902,535	115,85	-74,9	112	170	V	FAIL (*)
941,113	73,02	-32	316	170	V	FAIL (*)
947,455	69,5	-28,5	247	170	V	FAIL (*)
947,499	68,52	-27,5	313	170	V	FAIL (*)
Peak						
Frequency [MHz]	**Average [dBμV/m]**	**Margin [dB]**	**Azimuth [deg]**	**Height [cm]**	**Polar-isa-tion**	**SPR Result**
2707,114	58,19	5,8	45	170	V	PASSED

Table B.2: Phone C Radiated Spurious Emissions (GSM-900 On)

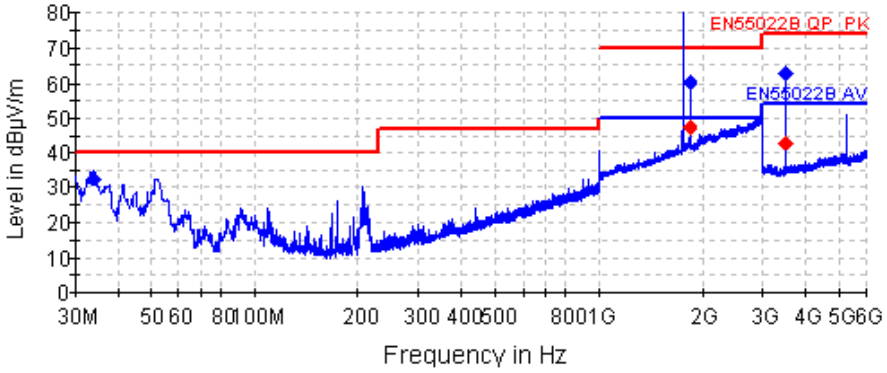

Figure B.3: Phone B Radiated Spurious Emissions (DCS-1800 On)

Average						
Frequency [MHz]	**Average [dBµV/m]**	**Margin [dB]**	**Azimuth [deg]**	**Height [cm]**	**Polar-isation**	**SPR Result**
1842,686	47,31	-3,3	47	170	V	FAIL (*)
3495,392	42,83	5,2	51	170	H	PASSED
Quasi-peak						
Frequency [MHz]	**Average [dBµV/m]**	**Margin [dB]**	**Azimuth [deg]**	**Height [cm]**	**Polar-isation**	**SPR Result**
33,878	32,49	1,5	58	170	V	PASSED
Peak						
Frequency [MHz]	**Average [dBµV/m]**	**Margin [dB]**	**Azimuth [deg]**	**Height [cm]**	**Polar-isation**	**SPR Result**
1842,686	60,16	3,8	47	170	V	PASSED
3495,392	62,74	5,3	51	170	H	PASSED

Table B.3: Phone B Radiated Spurious Emissions (DCS-1800 On)

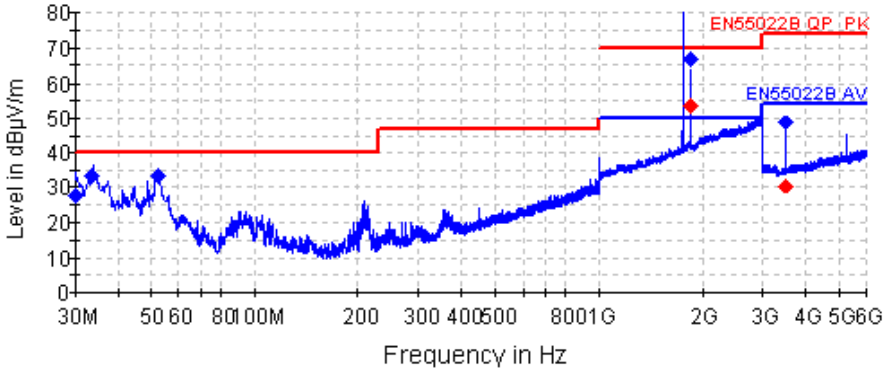

Figure B.4: Phone C Radiated Spurious Emissions (DCS-1800 On)

Average						
Frequency [MHz]	**Average [dBµV/m]**	**Margin [dB]**	**Azimuth [deg]**	**Height [cm]**	**Polar-isa-tion**	**SPR Result**
1848,897	53,79	-9,8	231	170	V	FAIL (*)
3495,79	30,47	17,5	89	170	H	PASSED
Quasi-peak						
Frequency [MHz]	**Average [dBµV/m]**	**Margin [dB]**	**Azimuth [deg]**	**Height [cm]**	**Polar-isa-tion**	**SPR Result**
30,36	27,83	6,2	343	170	V	PASSED
33,698	33,2	0,8	157	170	V	PASSED
52,285	33,49	0,5	96	170	V	PASSED
Peak						
Frequency [MHz]	**Average [dBµV/m]**	**Margin [dB]**	**Azimuth [deg]**	**Height [cm]**	**Polar-isa-tion**	**SPR Result**
1848,897	66,96	-3	231	170	V	FAIL (*)
3495,79	48,76	19,2	89	170	H	PASSED

Table B.4: Phone C Radiated Spurious Emissions (DCS-1800 On)

C. APPENDIX

Signal	Parameter	Limits (ns)		Phone C	
		Min	Max	Result (ns)	Pass
D/CX	Add setup time	0		1,7	Yes
D/CX	Add hold time (WR/RD)	10		59,8	Yes
WRX	Write Cycle	66		138,6	Yes
WRX	Control Pulse "H" duration	15		72,8	Yes
WRX	Control Pulse "L" duration	15		65,9	Yes
D(7..0)	Data setup time	10		44,9	Yes
D(7..0)	Data hold time	10		67,6	Yes
D(7..0)	Read access time (ID)		40	22,3	Yes

Table C.1: Interface timings for write function (Phone C).

Signal	Parameter	Limits (ns)		Phone B	
		Min	Max	Result (ns)	Pass
D/CX	Add setup time	0		1,7	Yes
D/CX	Add hold time (WR/RD)	10		60,4	Yes
WRX	Write Cycle	66		138,8	Yes
WRX	Control Pulse "H" duration	15		80,2	Yes
WRX	Control Pulse "L" duration	15		58,6	Yes
D(7..0)	Data setup time	10		-	-
D(7..0)	Data hold time	10		-	-
D(7..0)	Read access time (ID)		40	20,2	Yes

Table C.2: Interface timings for write function (Phone B).

Signal	Time	Limit	Phone C		Phone B	
			Result (ns)	Pass	Result (ns)	Pass
D/CX	Rise time	15 ns	11,1	Yes	11,0	Yes
D/CX	Fall time	15 ns	8,1	Yes	7,1	Yes
RDX	Rise time	15 ns	12,5	Yes	10,4	Yes
RDX	Fall time	15 ns	7,5	Yes	6,8	Yes
D0	Rise time	15 ns	10,4	Yes	-	-
D0	Fall time	15 ns	13,9	Yes	-	-
D1	Rise time	15 ns	7,8	Yes	-	-
D1	Fall time	15 ns	5,9	Yes	-	-
D2	Rise time	15 ns	7,0	Yes	7,6	Yes
D2	Fall time	15 ns	4,2	Yes	4,7	Yes
D3	Rise time	15 ns	8,0	Yes	7,7	Yes
D3	Fall time	15 ns	4,4	Yes	4,7	Yes
D4	Rise time	15 ns	7,6	Yes	7,4	Yes
D4	Fall time	15 ns	5,0	Yes	5,0	Yes
D5	Rise time	15 ns	7,8	Yes	8,0	Yes
D5	Fall time	15 ns	4,4	Yes	3,8	Yes
D6	Rise time	15 ns	8,0	Yes	8,3	Yes
D6	Fall time	15 ns	5,0	Yes	4,7	Yes
D7	Rise time	15 ns	9,0	Yes	9,0	Yes
D7	Fall time	15 ns	5,4	Yes	5,3	Yes
WRX	Rise time	15 ns	9,9	Yes	10,6	Yes
WRX	Fall time	15 ns	5,9	Yes	7,2	Yes

Table C.3: Signal rise and fall times of the display control lines.